Static Phenomena Near Critical Points: Theory and Experiment

LEO P. KADANOFF,* WOLFGANG GÖTZE,† DAVID HAMBLEN, ROBERT HECHT, E. A. S. LEWIS
V. V. PALCIAUSKAS, MARTIN RAYL, J. SWIFT

Department of Physics and *Materials Research Laboratory*,‡ *University of Illinois, Urbana, Illinois*

DAVID ASPNES

Department of Physics, Brown University, Providence, Rhode Island

JOSEPH KANE

The Laboratory of Atomic and Solid-State Physics, Cornell University, Ithaca, New York

This paper compares theory and experiment for behavior very near critical points. The primary experimental results are the "critical indices" which describe singularities in various thermodynamic derivatives and correlation functions. These indices are tabulated and compared with theory. The basic theoretical ideas are introduced via the molecular field approach, which brings in the concept of an order parameter and suggests that there are close relations among different phase transition problems. Although this theory is qualitatively correct it is quantitatively wrong, it predicts the wrong values of the critical indices. Another theoretical approach, the "scaling law" concept, which predicts relations among these indices, is described. The experimental evidence for and against the scaling laws is assessed. It is suggested that the scaling laws provide a promising approach to understanding phenomena near the critical point, but that they are by no means proved or disproved by the existing experimental data.

CONTENTS

I. INTRODUCTION

In recent years, considerable attention has been drawn to the phenomena which occur very near critical points. Several recent conferences[1,2] have presented a wealth of new experimental data and theoretical ideas in this area. These conferences have broadcast the fact that there are quite marked similarities between apparently very different phase transitions. An antiferromagnet near its Néel point behaves quite similarly to a liquid near its critical point. The superconducting transition is not very different from several ferroelectric transitions. In all cases, there is an apparently rather simple behavior in the region right around the critical point.

This simplicity and similarity among phase transitions is not fully elucidated theoretically. Some of the qualitative features of this behavior are reasonably well understood; others remain a complete mystery.

In this paper we review the present status of theory and experiment in this area, concentrating on the time-independent properties of systems near T_c. Thus, we look at thermodynamic derivatives and time-independent correlations but ignore the very interesting work on transport coefficients and time-dependent correlations. The particular subject is what can be learned by comparing different phase transitions with each other and with the existing theories. How are different phase transitions alike? In what ways do they differ? Why should we expect these similarities and differences?

Because we are considering such a broad range of phenomena, we cannot expect our readers to be experts in any particular area we describe. Consequently, we attempt to provide explanations and discussions which will be comprehensible to the nonexpert. We are hopeful that our treatment will provide some picture of the interrelations within this broad field.

In the next section, the important theoretical ideas—the order parameter, the choice between different phases, long-range correlations, and fluctuations—are introduced via the molecular field approximation. These results are tested by comparing them with

conclusions drawn from theoretical studies of the Ising model, which is a model of a ferromagnetic material that is particularly suitable for theoretical study. This comparison shows that the molecular field approximation gives a picture of the phase transition which is, at best, only qualitatively correct. The main quantitative predictions of the molecular field theory are a set of "critical indices" which turn out to have very different values from the indices found in the Ising model. In the third section we describe a recent theoretical proposal that there exist relations among the critical indices derived from the notion of "scaling laws".

In the next sections we turn successively to magnetic systems, critical points in classical liquids, the quantum liquid–gas phase transition, superfluids, and ferroelectrics. In each case, the experiments which determine the critical indices are tabulated and analyzed. These data are used to show many remarkable similarities between different phase transitions and a few equally remarkable differences. The relations among the indices predicted by the scaling laws are tested. Most often the theoretical ideas are supported by the experiments but the few discrepancies that exist allow one to leave open the question as to whether the scaling laws are in fact right.

II. MOLECULAR FIELD THEORIES

A. The Order Parameter

The most fundamental idea which helps elucidate the behavior near a critical point is the concept that this transition is describable by an order parameter.[3–5] This parameter, here indicated by the symbol $\langle p(\mathbf{r}) \rangle$, is a numerical measure of the amount and kind of ordering which is built up in the neighborhood of the critical point. For example, in a single domain ferromagnetic crystal with an easy axis of magnetization along the z direction, a suitable order parameter is the statistically averaged z component of the magnetization at the point $\mathbf{r}$, $\langle p(\mathbf{r}) \rangle = \langle M_z(\mathbf{r}) \rangle$. Besides indicating how much spin ordering there is, the order parameter defined in this way has the following important properties:

(a) It may vanish above the critical point but is must be nonzero in the region just below T_c.

(b) It can approach zero continuously at $T \rightarrow T_c$ from below. (For example, at zero applied field the magnetization vanishes as the temperature is raised to the Curie temperature.) This condition ensures that the transition not be of first order.

(c) Below the phase transition, the order parameter is not fully determined by the external conditions, but may take on two or more different values under physically identical conditions. For example, at zero applied magnetic field, the magnetization may point in the plus or minus z direction with equal facility

below T_c. Similarly, in the liquid–gas phase transition, the appropriate order parameter is the density minus the critical density, $\rho - \rho_c$. When liquid is in contact with vapor, this order parameter takes on two values: the positive value appropriate to the liquid phase and the negative value appropriate to the gaseous phase.

Table I lists a group of phase transitions which are of higher than first order—i.e., which can take place with zero latent heat—and gives the appropriate order parameter for each transition. Also included in this table are some indications of the amount of "free choice" which each $\langle p(\mathbf{r}) \rangle$ may have below T_c.[4] For future reference we also include in Table I a list of the variables which are the thermodynamic conjugate to the order parameter in each case. These conjugate variables are indicated in general by the symbol h.

B. The Landau Theory of the Second-Order Phase Transition—Thermodynamics

A relatively simple view of phenomena near the critical point was provided by Landau.[5] Although this theory does not agree quantitatively with experimental observations very close to the critical point, it does provide a qualitatively correct view of the kinds of things which do happen. Landau's theory is most easily discussed in the case of a ferromagnet with a small magnetic field, B, and T near T_c. Then the magnetization $M_z(\mathbf{r})$ is necessarily small and it would seem reasonable to expand the free energy in a power series in this magnetization. This expansion takes the following form

$$G = \int d^3r\, g(\mathbf{r}) \qquad (2.1)$$

with

$$g(\mathbf{r}) = g_0(T) - B_z(\mathbf{r}) M_z(\mathbf{r}) + a(T)[M_z(\mathbf{r})]^2$$
$$+ b(T)[M_z(\mathbf{r})]^4 + c(T)[\nabla M_z(\mathbf{r}) \cdot \nabla M_z(\mathbf{r})]. \quad (2.2)$$

The first term $g_0(T)$ represents the free energy per unit volume which would exist were there no magnetization. The second term $B_z M_z$ represents the direct interaction between the applied magnetic field **B**—assumed parallel to the easy axis z—and the magnetic moment of the spins within the sample. Direct spin–spin interactions produce the remaining terms in $g(\mathbf{r})$. Because these interactions do not change when we change the sign of M_z, these terms contain no odd powers of $M_z(\mathbf{r})$. This is the origin of the terms proportional to a and b in Eq. (2.2). The final term in this equation is inserted to make the free energy larger when $M_z(\mathbf{r})$ varies in space. Hence this term serves to damp out spatial variations in $M_z(\mathbf{r})$.

It is a general rule in statistical mechanics that the most probable value of any parameter is the one which minimizes the free energy. Thus, we would determine the most probable value of $M_z(\mathbf{r})$ by requiring that G

TABLE I. Partial list of transitions with critical points. In general, the symbol h denotes the conjugate to $\langle p \rangle$.

Transition	Meaning of $\langle p \rangle$	Free choice in $\langle p \rangle$	Thermodynamic conjugate of p
Liquid–gas	$\rho - \rho_c$	$p>0$=liquid $p<0$=vapor (2 choices)	μ
Ferromagnetic	magnetization $\langle \mathbf{M} \rangle$	if n equivalent "easy axes" $2n$ choices	applied magnetic field, H, along easy axes
Heisenberg model ferromagnet	magnetization $\langle \mathbf{M} \rangle$	direction of $\langle \mathbf{M} \rangle$ [can choose any value on surface of sphere.]	**H**
Antiferromagnet	sublattice magnetization	if n "easy axes" $2n$ choices	not physical
Ising model	$\langle \sigma_r \rangle$	2 choices	h
Superconductors	Δ (complex gap parameter)	phase of Δ	not physical
Superfluid	$\langle \psi \rangle$ (condensate wave function)	phase of $\langle \psi \rangle$	not physical
Ferroelectric	lattice polarization	finite number of choices	electric field
Phase separation	concentration	2 choices	a difference of chemical potentials

be stationary under the infinitesimal change

$$M_z(\mathbf{r}) \rightarrow M_z(\mathbf{r}) + \delta M_z(\mathbf{r}). \qquad (2.3)$$

The first-order change in G under this transformation is

$$\delta G = \int d^3 r \, \delta M_z(\mathbf{r})$$

$$\times \{ -B_z(\mathbf{r}) + 2aM_z(\mathbf{r}) + 4b[M_z(\mathbf{r})]^3 - 2c\nabla^2 M_z(\mathbf{r}) \}. \qquad (2.4)$$

Since this must vanish for all values of $\delta M_z(\mathbf{r})$, the brace must be zero. Hence the equation for the most probable value of $M_z(\mathbf{r})$ is

$$\{ 2a + 4b[M_z(\mathbf{r})]^2 - 2c\nabla^2 \} M_z(\mathbf{r}) = B_z(\mathbf{r}). \qquad (2.5)$$

Landau now makes the drastic assumption of neglecting all fluctuations in the magnetization. This is equivalent to the assertion that the most probable value of the magnetization, as defined by Eq. (2.5), is the only value and hence also the mean value.

The free energy is obtained by solving (2.5), and then substituting the solution into (2.2). When there is ambiguity arising from multiple solutions to (2.5), this is to be resolved by choosing the solution which actually minimizes G. For this procedure to work, b and c must both be greater than zero; otherwise there is no minimum for G. (If $b<0$, the transition is first order; if $c<0$ the magnetization is never uniform.)

Begin with the simplest case, that in which $B_z(\mathbf{r})$ is independent of $\mathbf{r}$. Then there is no reason for spatial

variation of $M_z(\mathbf{r})$ and (2.5) reduces to

$$[2a + 4bM_z^2]M_z = B_z. \qquad (2.6)$$

When $B_z = 0$ this has the solutions

$$M_z = 0 \qquad (2.7a)$$

$$M_z = \pm(-a/2b)^{1/2}. \qquad (2.7b)$$

The first solution (2.7a) actually minimizes the free energy when $a>0$; the remaining solutions (2.7b) minimize G when $a<0$. But since we want the magnetization at $B_z = 0$ to vanish above T_c and to be nonzero below T_c, we must have

$$a>0 \qquad \text{for } T>T_c$$

$$a<0 \qquad \text{for } T<T_c.$$

Landau chooses the simplest form of $a(T)$ which will accomplish this purpose: he takes

$$a(T) = a'(T - T_c) \qquad (2.8)$$

near T_c. He also guesses that b and c approach constants as $T \rightarrow T_c$. This choice of $a(T)$ ensures that at the critical point ($B_z = 0$, $T = T_c$) the system can produce a nonzero magnetization with a cost in free energy which is of fourth order in M_z. Hence near T_c the system can produce large-scale fluctuations in the order parameter with relatively little cost in free energy. According to the best present beliefs this unusual susceptibility to fluctuations is the cause of all the special phenomena which appear near the critical point.

TABLE II. Parameters describing phase transition.

Physical quantity	Range of variables $\epsilon = (T-T_c)/T_c$	h	Behavior of quantity	Parameter describing quantity
$\langle p \rangle$	>0	0	$\langle p \rangle = 0$	
	<0	0	$\langle p \rangle \sim \pm \lvert \epsilon \rvert^\beta$	β
	0	$\neq 0$	$\sim \pm \lvert h \rvert^{1/\delta}$	δ
$\chi = \partial \langle p \rangle / \partial h \rvert_\epsilon$	>0	0	$\sim \epsilon^{-\gamma}$	γ
	<0	0	$\sim \lvert \epsilon \rvert^{-\gamma'}$	γ'
$g(r, r') = \langle p_r p_{r'} \rangle - \langle p \rangle^2$	0	0	$\sim \lvert r-r' \rvert^{-d+2-\eta}$	η
ξ = range of $g(r, r')$	>0	0	$\sim \epsilon^{-\nu}$	ν
	<0	0	$\sim \epsilon^{-\nu'}$	ν'
C_h = specific heat at constant h	>0	0	$a\epsilon^{-\alpha} + b$	α
	<0	0	$a' \lvert \epsilon \rvert^{-\alpha'} + b'$	α'
or	>0	0	$A \log \epsilon^{-1} + B$	$\alpha = 0$
	<0	0	$A' \log \lvert \epsilon \rvert^{-1} + B'$	$\alpha' = 0$

We now follow the thread of the Landau theory and derive the relation between critical phenomena and fluctuations from the free-energy formulation of Eqs. (2.2) and (2.5). The reader will recognize that there is a physical inconsistency in this whole calculation. Equation (2.5) was obtained by neglecting fluctuations —and we shall finally conclude that fluctuations are all-important! But the Landau theory, although it is essentially inconsistent near T_c, does give a good indication of the kind of behavior to be expected.

First, look at the temperature dependence of $\langle p(\mathbf{r}) \rangle$ (the magnetization) at zero h (magnetic field). According to (2.7b) and (2.8) the magnetization just below T_c is proportional to $(T_c - T)^{1/2}$. Since we shall obtain and use several results of this type, it is convenient to collect them in tabular form. In the second line of Table II, we define an index β by the condition that the order parameter go to zero as $(T_c - T)^\beta$ when the thermodynamic conjugate to the order parameter h, is at its critical value.

We have just concluded that in the Landau theory $\beta = \frac{1}{2}$, as given in the first entry in Table III.

To continue this compilation, take Eq. (2.6) at $T - T_c = 0$. Then $a = 0$ so that Eq. (2.6) implies

$$M_z = \{B_z/4b\}^{1/\delta} \quad \text{with} \quad \delta = 3. \qquad (2.9)$$

This gives the next entries in Tables II and III.

The susceptibility, $\chi = (\partial M_z / \partial B)_T$ is calculated by differentiating Eq. (2.6) with respect to B. At zero magnetic field, the resulting susceptibility may be evaluated above and below T_c by employing respectively Eqs. (2.7a) and (2.7b). In the end the magnetic susceptibility is seen to diverge both above and below T_c as $\lvert T - T_c \rvert^{-1}$. Hence the values $\gamma = \gamma' = 1$ are recorded in Table III.

The final thermodynamic property which we will obtain from the Landau theory is the specific heat at zero magnetic field, which is given by thermodynamics as

$$T^{-1}C_B = -\partial^2 G/\partial T^2 \rvert_{B=0}. \qquad (2.10)$$

But, at $B=0$, we can use (2.7) to find

$$G = \int d\mathbf{r}[g_0(T)] \qquad \text{for } T > T_c$$

$$= \int d\mathbf{r}[g_0(T) - (a^2/4b)] \qquad \text{for } T < T_c. \qquad (2.11)$$

This extra term in the free energy below T_c produces, when it is twice differentiated, a constant term in the specific heat. Thus, there is a discontinuity in the specific heat at T_c predicted by the Landau theory.

C. Landau Theory—Fluctuations

Next consider fluctuations in the magnetization $M_z(\mathbf{r})$. These fluctuations are given by $[M_z(\mathbf{r}) - \langle M_z(\mathbf{r}) \rangle]$. The point to be studied is how the deviation of M_z from its average at one point in the material is tied to the similar fluctuations in neighboring regions. The mathematical description of this correction is given by the correlation function $g(\mathbf{r}, \mathbf{r}')$ defined by

$$g(\mathbf{r}, \mathbf{r}')$$
$$= \langle [M_z(\mathbf{r}) - \langle M_z(\mathbf{r}) \rangle][M_z(\mathbf{r}') - \langle M_z(\mathbf{r}') \rangle] \rangle. \qquad (2.12)$$

At first sight it is hard to see how g can be calculated within the context of the Landau theory. The difficulty arises because this theory begins by neglecting fluctuations, i.e., by saying that $M_z(\mathbf{r}) - \langle M_z(\mathbf{r}) \rangle$ is very small. Now we wish to use the theory in order to calculate a first correction to this initial statement.

Fortunately there is a well-defined procedure for calculating correlation functions starting from the free energy. This procedure arises from a quite general

TABLE III. Comparison of Landau theory and Ising models.[a]

Physical quantity	Parameter	Landau theory	Ising model	
			2-D	3-D
$\langle p \rangle$	β	1/2	1/8	0.313 ± 0.004
	δ	3	15	5.2 ± 0.15
χ	γ	1	7/4	1.250 ± 0.001
	γ'	1	7/4	1.31 ± 0.05
$g(r, r')$	η	0	1/4	0.056 ± 0.008
ξ	ν	1/2	1	0.643 ± 0.0025
	ν'	1/2	1	?
C_h	α	0	0	$0.0 \leq \alpha \leq 0.25$
	α'	discontinuity in C_h 0	log ∞ in C_h 0	$0.066 + 0.16, -0.04$

theorem of *classical* statistical mechanics. This theorem[6] states that if the Hamiltonian contains the parameter $h(\mathbf{r})$ in the combination

$$-\int d\mathbf{r} h(\mathbf{r}) p(\mathbf{r}) \qquad (2.13)$$

then if we allow $h(\mathbf{r})$ to change by adding to it the small increment $\delta h(\mathbf{r})$, this change induces a change in $\langle p(\mathbf{r}) \rangle$, which is

$$\delta \langle p(\mathbf{r}) \rangle = (kT)^{-1} \int d\mathbf{r}' \langle [p(\mathbf{r})) - \langle p(\mathbf{r}) \rangle]$$

$$\times [p(\mathbf{r}') - \langle p(\mathbf{r}') \rangle] \rangle \delta h(\mathbf{r}'). \qquad (2.14)$$

Here k is the Boltzmann constant. In our case $h(\mathbf{r})$ corresponds to the magnetic field, $p(\mathbf{r})$ to the magnetization, and (2.14) reads

$$\delta \langle M_z(\mathbf{r}) \rangle = (kT)^{-1} \int d\mathbf{r}' g(\mathbf{r}, \mathbf{r}') \delta B_z(\mathbf{r}'). \qquad (2.15)$$

Our equation for the average magnetization in the Landau theory is (2.5). If we calculate the first-order change in that equation as $B_z(\mathbf{r}) \rightarrow B_z(\mathbf{r}) + \delta B_z(\mathbf{r})$ so that $M_z(\mathbf{r}) \rightarrow M_z(\mathbf{r}) + \delta M_z(\mathbf{r})$ we find that (2.5) implies

$$\{2a + 12b \langle M_z(\mathbf{r}) \rangle^2 - 2c \nabla^2\} \delta \langle M_z(\mathbf{r}) \rangle = \delta B_z(\mathbf{r}). \qquad (2.16)$$

Next, substitute (2.15) into (2.16) and move $\delta B_z(\mathbf{r})$ to the left-hand side of the equation to find

$$\int d\mathbf{r}' \{[2a + 12b \langle M_z(\mathbf{r}) \rangle^2 - 2c \nabla^2] g(\mathbf{r}, \mathbf{r}') - kT \delta(\mathbf{r} - \mathbf{r}')\}$$

$$\times \delta B(\mathbf{r}') = 0.$$

Since $\delta B(\mathbf{r}')$ is arbitrary, the entire brace must vanish and the correlation function therefore obeys the

equation

$$[2a + 12b \langle M_z(\mathbf{r}) \rangle^2 - 2c \nabla^2] g(\mathbf{r}, \mathbf{r}') = kT \delta(\mathbf{r} - \mathbf{r}'). \qquad (2.17)$$

Equation (2.17) is easily solved when the magnetic field is zero. In this case, for $T > T_c$ the average magnetization vanishes and (2.17) reduces to

$$[2a'(T - T_c) - 2c \nabla^2] g(\mathbf{r}, \mathbf{r}') = kT \delta(\mathbf{r} - \mathbf{r}')$$

$$\text{for } T > T_c. \qquad (2.18a)$$

For $T < T_c$ the squared magnetization is proportional to $T_c - T$ according to (2.7b) so that (2.17) becomes

$$[4a'(T_c - T) - 2c \nabla^2] g(\mathbf{r}, \mathbf{r}') = kT \delta(\mathbf{r} - \mathbf{r}'). \qquad (2.18b)$$

In three dimensions these equations have the solution

$$g(r, r') = \frac{\exp(-|\mathbf{r} - \mathbf{r}'|/\xi)}{|\mathbf{r} - \mathbf{r}'|} \frac{kT}{8\pi c} \qquad (2.19)$$

with

$$\xi = (c/a')^{1/2}(T - T_c)^{-1/2} \qquad \text{for } T > T_c$$

$$\xi = (c/2a')^{1/2}(T_c - T)^{-1/2} \qquad \text{for } T < T_c. \qquad (2.20)$$

Before discussing the consequences of (2.19), we must indicate why a g determined from the theorem of classical statistical mechanics [Eq. (2.15)] is correct for this quantum-mechanical problem. Equation (2.19) is not correct for all values of $(\mathbf{r} - \mathbf{r}')$, because quantum-mechanical fluctuations do, in fact, invalidate the derivation. But, when $|\mathbf{r} - \mathbf{r}'|$ is much greater than a lattice constant, we can replace the magnetization by its average over several cells of the lattice. Since this magnetization is now produced by many spins quantum fluctuations become insignificant. Hence the result (2.19) is a correct consequence of the Landau theory. whenever $|\mathbf{r} - \mathbf{r}'|$ is much bigger than a lattice constant.

But the important fact is that the correlation function (2.19) has such a very large spatial range near T_c. As T approaches T_c its characteristic range ξ

grows as $|T-T_c|^{-\nu}$, where $\nu=\frac{1}{2}$ in the Landau theory. This range measures the typical size of a region in which a coherent fluctuation in the magnetization occurs. As we get closer to the critical point, these fluctuations cover more space. Finally, at the critical point the spatial extend of the correlation functions becomes infinite and then g drops off very slowly in space. In three dimensions this drop-off occurs as $|r-r'|^{-1}$. In the general case of a d-dimensional lattice, the Landau theory predicts a drop-off as $|r-r'|^{-(d-2)}$.

All of the conclusions of this and the preceding section are consequences of the simple assumption that the free energy is expandable in power series in the order parameter and in $(T-T_c)$. A large number of theories of phase transitions make implicit use of this assumption. All of these approaches must necessarily lead to the same conclusions as Landau's about behavior near the critical point. In particular, they give the same values of the critical indices α, β, γ, δ, η, and ν. Examples of theories which are equivalent to Landau's are the van der Waals' equation for a liquid, the Weiss molecular field theory for a ferromagnet and its variants which have been applied to a variety of other systems, the Ornstein–Zernike equations for g, many varieties of the random phase approximation,[7] the Ginzburg–Landau equations for superconductors,[8] etc. Many of these approaches give correct information far from the critical point; but they all are expected to fail as the critical point is closely approached.

D. Connections Between Correlation Functions and Thermodynamics

All of these calculations do include some qualitatively correct statements. One is that large-scale fluctuations in the order parameter are the source of the singularities in thermodynamic derivatives near the critical point. To understand this point, refer back to Eq. (2.15) which gives an exact formula for the change in magnetization produced by a change in magnetic field in terms of a correlation function. If the change in magnetic field is independent of r, Eq. (2.15) then gives the thermodynamic response of the magnetization to a change in B_z. This is precisely a definition of the magnetic susceptibility. Hence Eq. (2.15) implies that the susceptibility is

$$\chi \equiv \partial M_z/\partial B_z \mid_T = \delta M_z/\delta B_z$$

$$= (kT)^{-1}\int dr' g(r, r'). \qquad (2.21)$$

As $T\to T_c$ the range of the correlation function increases. Hence the r' integral covers a larger and larger region and the integral goes to infinity at T_c. Hence the divergence in the range of correlations is the precise cause of this and all the other singularities in thermodynamic derivatives.

It is possible to follow this point explicity through in the context of the Landau theory. Simply substitute the form (2.19) for g into (2.21) and perform the integral. Then, it follows that the susceptibility is, at $B=0$

$$\chi = (2c)^{-1}\xi^2. \qquad (2.22)$$

This result shows directly how a divergence in the range of correlations may produce a divergence in a thermodynamic derivative.

There are other useful exact correlation function expressions for thermodynamic derivatives. For example, if $E(r)$ is the energy density, the specific heat at fixed B is given by

$$C_B = \frac{1}{kT^2}\int dr' \langle [E(r)-\langle E(r)\rangle][E(r')-\langle E(r')\rangle]\rangle \qquad (2.23a)$$

and also

$$T[\partial \langle M_z(r)\rangle/\partial T]\mid_{B_z}$$

$$= \partial \langle E(r)\rangle/\partial B_z \mid_T$$

$$= (kT)^{-1}\int dr' \langle [E(r)-\langle E(r)\rangle]$$

$$\times [M_z(r')-\langle M_z(r')\rangle]\rangle. \qquad (2.23b)$$

E. The Ising Model

In order to investigate the correctness of the Landau theory we quote results from theoretical investigations of the Ising model. This is essentially a very anisotropic ferromagnet in which only the z components of the spins are coupled. The spins are denoted by σ_r where r gives the position on the lattice. Each σ_r can take on the values ± 1. Then the Hamiltonian is given by

$$H/kT = -h\sum_r \sigma_r - K\sum_{r,r'}\sigma_r\sigma_{r'}. \qquad (2.24)$$

The first term in H represents an interaction with an external "magnetic field" h, which tends to make the spins point up if h is positive and down if h is nagative. The second term is an interaction among spins which, when K is positive, tends to line up neighboring spins with each other. To keep the interaction short-ranged, the second sum is carried out only over r and r' which are nearest neighbors.

To calculate the statistical mechanics of the Ising model it is necessary to compute the free energy, G, which is given by

$$\sum \exp(-H/kT) = \exp(-G/kT). \qquad (2.25)$$

Here, the sum covers all possible values of the σ_r. That is, if there are N sites on the lattice, the sum has 2^N terms.

Some of the qualitative features of the resulting partition function are rather easy to guess on physical grounds. For example, consider the average "magnetiza-

tion," $\langle\sigma_r\rangle$, which is proportional to $(\partial G/\partial h)\mid_T$. At zero temperature and $h=0$, the aligning force represented by K wins out and the spins are perfectly aligned. Then (see Fig. 1), $\langle\sigma_r\rangle$ is either plus or minus unity. As the temperature is increased, with h held equal to zero, the magnitude of $\langle\sigma_r\rangle$ continually decreases until, at a critical temperature T_c, it disappears completely. Any applied field, h, will tend to increase the alignment, i.e., $\mid\langle\sigma_r\rangle\mid$. This, too, is indicated in Fig. 1.

Onsager[9] calculated the sum (2.25) in two dimensions at $h=0$ and others have extended his work to get other physical properties.[10–12] The results have been described in review articles[13] and monographs.[3,14] This theory gives the values of all the critical indices defined in Table II except for δ. These theoretical values of critical indices are listed in Table III.

In three dimensions, there is no general solution. But there do exist numerical ways of attacking this problem. Various physical quantities can be expanded in power series about $T=0$ and about $T=\infty$. Then, there exist numerical tricks for guessing the radius of convergence of these power series and even their behavior near singularities. From this emerges numerical estimates for the parameters of the two-and three-dimensional Ising models. Table III records the values of the critical indices obtained from these numerical calculations. These are mostly taken from reviews of Fisher.[1,15–17]

The validity of these numerical methods may be checked by comparing the results with the exact two-dimensional calculations based upon the Onsager solution. It is found that the methods generally work well, except that occasionally the convergence is uncomfortably slow. The estimate of α' is, for example, not as accurate as we would like. On the other hand, γ is known to one part in a thousand for the sc, fcc, bcc, and diamond lattices.[15] According to these numerical estimates, the values of the parameters are, as far as we can tell, independent of the detailed nature of the lattice.

Table III reveals that the Ising model behaves very differently from the predictions of the Landau theory. Thus, for example, the specific heat is discontinuous in the Landau approach but has a logarithmic infinity in the two-dimensional Ising model and an infinity which is probably stronger than logarithmic in three dimensions. As another example, $\beta=\frac{1}{8}$ in the two-dimensional Ising model and is close to 0.31 in three dimensions; these results are clearly different from the $\beta=\frac{1}{2}$ predicted by the simple theory.

Because exact solutions exist for the two-dimensional Ising model at $h=0$ it is possible to calculate several of the relevant correlation functions in this case. For example, it is possible to show that the spin–spin correlation function has a relatively simple form in the case in which T is close to T_c and the spins are separated by a large distance. To express this result
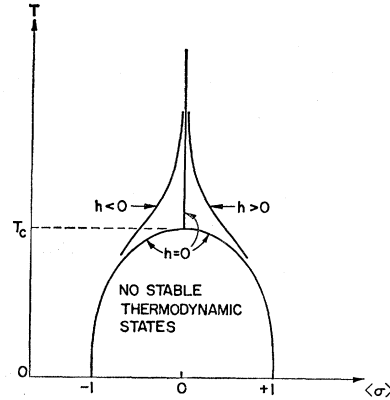

FIG. 1. Magnetization vs temperature (schematic) for various values of h. Below the $h=0$ curve, there are no stable thermodynamic states.

we use the variable

$$\epsilon = (T-T_c)/T_c \qquad (2.26)$$

which is a dimensionless measure of the deviation from the critical temperature and

$$R = \mid r-r'\mid /(\text{lattice constant}). \qquad (2.27)$$

When $\epsilon\ll1$, $R\gg1$, but ϵR arbitrary, the spin–spin correlation function has the structure[11]

$$g(r, r') = \mid\epsilon\mid^{1/4}G(\epsilon R). \qquad (2.28a)$$

The corresponding results for the energy density-energy density correlation function and the energy density–spin correlation function are, under the same restrictions for ϵ and R,[18]

$$\langle[E(r)-\langle E\rangle][E(r')-\langle E\rangle]\rangle = \mid\epsilon\mid^2 G_{EE}(\epsilon R)$$

$$(2.28b)$$

$$\langle[\sigma(r)-\langle\sigma\rangle][E(r')-\langle E\rangle]\rangle = \mid\epsilon\mid^{1+1/8} G_{\sigma E}(\epsilon R),$$

$$(2.28c)$$

where $G_{\sigma E}(\epsilon R)$ happens to vanish for all positive values of its argument, i.e., for all $T>T_c$.

Several interesting facts can be learned from these correlation functions. First, consider their values for large spatial separations between the points, i.e., for $\epsilon R\gg1$. In this limit, each of the correlation functions decreases exponentially. The spin–spin correlation function behaves as[11]

$$g(r, r')\sim[\epsilon^{1/4}/(\epsilon R)^{1/2}]\exp(-\mid\epsilon\mid R)$$

$$\text{for } T>T_c \quad (2.29a)$$

and

$$g(r, r')\sim[\mid\epsilon\mid^{1/4}/(\epsilon R)^2]\exp(-2\mid\epsilon\mid R)$$

$$\text{for } T<T_c \quad (2.29b)$$

while the energy density–energy density correlation function behaves as[18]

$$[\epsilon^2/(\epsilon R)^2] \exp\,(-2\,|\,\epsilon\,|\,R) \qquad (2.29c)$$

and the energy density–spin correlation function has the behavior[18] for $\epsilon < 0$

$$[|\,\epsilon\,|^{\,1+1/8}/(\epsilon R)^2] \exp\,(-2\,|\,\epsilon\,|\,R). \qquad (2.29d)$$

Hence in this limit all three correlation functions go exponentially to zero with the same characteristic range

$$\xi \sim |\,\epsilon\,|^{\,-1}. \qquad (2.30)$$

These correlation functions each reduce to a simple form when $\epsilon \to 0$. In this case even though R is very large ϵR is very small. Hence the functions in (2.28) are evaluated for small values of their arguments. Then the spin–spin correlation function takes the form[19]

$$g(\mathbf{r}, \mathbf{r}') \sim R^{-1/4} \qquad (2.31a)$$

the energy density–spin correlation function becomes proportional to

$$\langle \sigma \rangle / R \qquad (2.31b)$$

where the energy density–energy density correlation function becomes proportional to[18]

$$R^{-2}. \qquad (2.31c)$$

By using these results, we can see again how the divergences in thermodynamic derivatives are connected with the very long range of the correlation functions. For example, the specific heat at constant B according to (2.23) is proportional to the spatial intergral of the energy density–energy density correlation function. In the region

$$1 \ll R \ll (\xi/a_0),$$

where a_0 is the lattice constant Eq. (2.31c) gives the appropriate form for this correlation function. Hence this region contributes a part

$$\int_{\sim 1}^{\sim \xi/a_0} d^2R/R^2 \sim 2\pi \int_1^{\xi/a_0} \frac{dR}{R} \sim 2\pi \log\,(\xi/a_0) \qquad (2.32)$$

to the specific heat. Since the correlation function decreases very sharply as R becomes much bigger than ξ, Eq. (2.32) gives a correct estimate of the temperature dependence of the specific heat. From the fact that $\xi \sim |\,\epsilon\,|^{-1}$, we then infer the logarithmic divergence of the specific heat.

We expect that the long-ranged correlations are relatively insensitive to the details of the interactions between spins. If a correlation extends over a hundred or a million lattice constants, this correlation should be sensitive only to the grossest features of the interaction and should not be affected by a change from a bcc to a fcc lattice or to the introduction of some next-nearest-neighbor interaction. The Ising model solutions do, in fact, bear this out. The correlations in the

two-dimensional case are basically the same for square and triangular lattices. In the three-dimensional case, so far as we can tell, $\gamma = 1.25$ equally well for bcc, fcc, and simple cubic lattices.

F. Range of Validity of Landau Theory

Now that we have seen that the Landau theory does not work for Ising models, we ask when we expect this theory to work at all. Ginzburg[20] has proposed an argument which uses the Landau theory to predict its own range of validity. To do this, consider fluctuations in the order parameter—which we assumed small. Actual order parameters, e.g., the magnetization in a ferromagnet, fluctuate considerably. However, some of these fluctuations may be removed by averaging the order parameter over a suitable region of space. This averaging, however, cannot cover too large a region without ruining the local nature of the Landau theory of the second-order phase transition. The largest range over which we can average without ruining the theory is the coherence distance ξ.

Thus, for the Landau theory to be valid, fluctuations in the order parameter over distances comparable with ξ must be relatively small. In particular, they must be small in comparison with the order parameter itself. We must have then,

$$\langle [p(\mathbf{r}) - \langle p \rangle][p(\mathbf{r}') - \langle p \rangle] \rangle \,|\,_{|\mathbf{r}-\mathbf{r}'|\sim\xi} \ll \langle p \rangle^2, \qquad (2.33)$$

where we are now using the symbol $\langle p(\mathbf{r}) \rangle$ for the order parameter. We estimate the right- and left-hand sides of (2.33) below T_c at zero magnetic field from Eqs. (2.19) and (2.7b). The result is that this necessary condition for the validity of the Landau theory becomes

$$kT_c/4\pi ec\xi(T) \ll -a/b. \qquad (2.34)$$

We can rewrite this in terms of more physical quantities by using Eq. (2.20) for $\xi(T)$. We then extrapolate this expression to $T = 0$, and define an extrapolated zero temperature coherence length

$$\lambda = (c/2a'T_c)^{1/2} \qquad (2.35)$$

so that the true correlation length of the Landau theory is, near T_c,

$$\xi(T) = \lambda\,|\,\epsilon\,|^{-1/2}. \qquad (2.36)$$

The jump in the heat capacity per unit volume (at $B = 0$) predicted by the Landau theory is

$$\Delta C = [(a')^2/2b]T_c. \qquad (2.37)$$

In terms of these physical quantities (2.34) reads

$$[16\pi e(\Delta C/k)\lambda^3]^{-1} \ll |\,\epsilon\,|^{1/2}. \qquad (2.38)$$

Ginzburg[20] and Levanyuk[21] produced somewhat more careful versions of this argument. They came to the conclusion that the Landau theory could only be correct if $|\,\epsilon\,|$ were much greater than a critical value,

$$\epsilon_c = (1/32\pi^2)\,(k/\Delta C\lambda^3)^2. \qquad (2.39)$$

When $|\epsilon| \ll \epsilon_c$, fluctuations become important and the molecular field theories all fail. For $1 \gg |\epsilon| \gg \epsilon_c$, we expect these theories to be valid. This calculation of ϵ_c is just an order of magnitude argument so one should, perhaps, not take the $32\pi^2$ in the denominator of Eq. (2.39) too seriously.

The factor λ^6 in the denominator of ϵ_c indicates that as the range of the forces, and hence the range of zero temperature correlations, gets longer and longer the Landau theory gets better and better. This point has been made explicitly in several recent papers[22-24] which show explicitly that the van der Waals theory (which is equivalent to Landau's near T_c) follows rigorously when you have an infinite range interaction.

Let us discuss ϵ_c for some examples:

Superconductors

For pure superconductors we expect λ to be of the same order as the zero temperature coherence length ξ_0. In tin,[25] $\xi_0 = 2300$ Å and $\Delta C = 0.8 \times 10^4$ ergs/cm^{-3} deg^{-1}. Therefore, Eq. (2.39) would indicate that deviations from the molecular field theory (which is, in this case, the Ginzburg–Landau[8] theory) should not be expected until ϵ gets as small as 10^{-14}. This very small value of ϵ_c arises because of the very long range of coherence in the superconductor. Similar results for the width of the critical region have been obtained by several other authors, who have carried out more detailed calculations of the dependence of specific heat[26] and electrical resistance[27] upon ϵ.

The Superfluid

In the λ transition of liquid He[4], the situation is very different. The $T=0$ coherence length is quite comparable with the interatomic spacing instead of the huge number encountered in the superconducting transition. Consequently, there appears to be no region at all in which the molecular field theory is satisfactory.

Magnetic Transitions

In the case of iron ΔC is about 3×10^7 ergs cm^{-3} deg^{-1}. Here ξ can be measured directly by neutron scattering experiments. The total cross section σ for momentum $\hbar k$ is proportional to $(\xi^{-2}+k^2)^{-1}$. The experimental value for λ is about 2 Å[28] so that $\epsilon_c \sim 10^{-2}$.

However, there is some experimental indication that the molecular field theory might be accurate for small values of ϵ, below T_c.[29,30] This might occur because for small ϵ, the weak magnetic dipole interactions between spins may become important. Since these interactions have a long range, the molecular field theory might perhaps again become correct in some range that includes small values of ϵ.

Since the magnetic fields produced by the spins in an antiferromagnet tend to cancel out, the magnetic interaction effectively has a much shorter range in an antiferromagnet. There is, then, no reason to expect
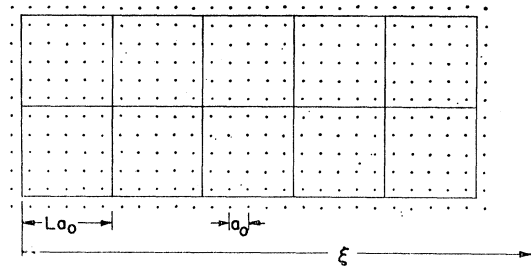

FIG. 2. Division of Ising model lattice into cells. $L \gg 1$ but $La_0 \ll \xi$.

molecular field theory to be correct for small ϵ in an antiferromagnet.

Ferroelectrics

Ginzburg[20] has estimated λ for BaTiO$_3$ and uses Eq. (2.39) to find $\epsilon_c \sim 10^{-4}$. The reason for this small value is that it is the smoothly varying coulomb force which is responsible for establishing the ferroelectric phase. Thus, in this case, the molecular field theory is expected to work for all $|\epsilon| \gg 10^{-4}$. However, in the antiferroelectric, one should not expect a similar preservation of molecular field theory. The experimental data partially support this point of view since the only observation of γ different from the molecular field result ($\gamma = 1$) is in the antiferroelectric phase of Rochelle salt.

III. SCALING LAWS

A. Formulation

Ideally, theory should predict values of the critical parameters, α, α', β, γ, γ', δ, ν, ν', and η. But, except for the case of the two-dimensional Ising model, no analytical theory exists.

A series of recent proposals[31-38] suggest that there exist relations among these indices, in particular, that there are not nine unknown quantities, but instead that the nine critical indices can all be expressed in terms of two fundamental unknown indices. There have been several suggested "derivations" of these relations among the critical indices. None really derive all the results at hand; they are plausibility arguments.

To see one of these consider an Ising model lattice. Imagine that we mentally divide the lattice into cells, each side of length La_0, where a_0 is the lattice constant. L is chosen to be very small compared to a coherence length, but is large enough so that the cell contains many spin sites (see Fig. 2).

$$1 \ll L \ll \xi/a_0. \qquad (3.1)$$

Let us assume for a moment that all the interactions between different cells were turned off. Then each cell would act independently of every other and there would be no correlations over distances larger

than a cell size. But, these are precisely the correlations which produce the divergences in thermodynamic derivatives which are characteristic of the critical region. Hence correlations between different cells must be quite crucial—the interactions among cells must be all important.[39]

We have already noted that the correlations near the critical point should not depend upon the details of the interaction. Let us assume that the cell size La_0 is one of these irrelevant details. Then, in each cell there must be a variable μ_a, a being a label for the cell, which behaves in an essentially identical fashion to our original variable σ_r. That is, interactions among different cells should produce correlations among the μ_a's identical in structure to the correlations in the original Ising model problem.[40]

The only possible difference between the site problem and the cell problem can be in the values of the two parameters ϵ and h. Assume that the values of these parameters for the cell problem are $\tilde{\epsilon}$ and $\tilde{h}$. Since these, respectively, describe the crucial effects of the interactions among cells and the interaction between each cell and the external magnetic field, they can depend upon the size of the cell. As the magnetic field goes to zero, the effective field in the cell problem must also go to zero. Hence $\tilde{h} \sim h$. The constant of proportionality may depend on the cell size so we guess

$$\tilde{h}= L^x h, \tag{3.1a}$$

where x is unknown. Similarly guess

$$\tilde{\epsilon}= L^y \epsilon, \tag{3.1b}$$

so that the cell problem will become critical as the site problem becomes critical. It follows that all nine critical indices may be determined in terms of x and y.

B. Thermodynamic Results

First we calculate the change in the free energy as h changes by an infinitesimal amount. Assume the h_r varies so slowly with r that the field may effectively be considered constant in each cell. Then the change in the free energy is

$$\delta(G/kT) = -\sum_r \langle\sigma_r\rangle\delta h_r = -\sum_a \langle\mu_a\rangle\delta\tilde{h}_a. \tag{3.2}$$

This must be the same in the two problems because this change in the free energy is a physical quantity. But, since the variation in space is assumed to be very slow we can replace the sum over cells r by the number of sites per cell times a sum over cells. This number is just L^d, where d is the dimensionality of the system.

Thus, (3.2) implies

$$L^d\langle\sigma_r\rangle\delta h_r= \langle\mu_a\rangle\delta\tilde{h}_a. \tag{3.3}$$

From (3.1a) and (3.3) it follows that

$$\sigma_r= L^{x-d}\mu_a. \tag{3.4}$$

Next calculate $\langle\sigma_r\rangle$ for the case in which the field h_r does not depend upon r. This depends upon ϵ and h,

$$\langle\sigma_r\rangle= F(\epsilon, h). \tag{3.5a}$$

Since μ_a is supposed to describe a problem identical to the original one except that it has new values of ϵ and h, $\langle\mu\rangle$ is the *same* function of the *new* variables

$$\langle\mu\rangle= F(\tilde{\epsilon}, \tilde{h}). \tag{3.5b}$$

Equations (3.2), (3.4), and (3.5) now combine as

$$\langle\sigma\rangle= F(\epsilon, h) = L^{x-d}F(L^y\epsilon, L^x h). \tag{3.6}$$

But the length L is only a mathematical construct. It must cancel out of the right-hand side of (3.6). This can only happen if $F(\epsilon, h)$ is of the form

$$\langle\sigma\rangle= F(\epsilon, h) = (h/|h|) |\epsilon|^{(d-x)/y} f(\epsilon/|h|^{y/x}). \tag{3.7}$$

The factor $h/|h|$ in (3.7) is inserted to ensure that $\langle\sigma\rangle$ changes sign as the sign of the magnetic field is changed.[41]

The functional form of the $f(z)$ defined by (3.7) is not known to us. Nevertheless, (3.7) permits us to compute critical indices in terms of x and y. For example, if $\langle\sigma\rangle\sim|\epsilon|^\beta$ for small negative ϵ, it must be true that $f(-\infty) = $ const. Then (3.7) gives

$$\beta= (d-x)/y. \tag{3.8}$$

All other thermodynamic derivatives may be found by differentiating or integrating $\langle\sigma\rangle$ with respect to ϵ and h. Thus α, α', γ, γ', and δ may be expressed in terms of x and y. The result is that the six indices in question are expressed in terms of the two parameters, or alternatively, the six indices obey four relations. These are[42]

$$\gamma=\gamma', \tag{3.9a}$$

$$\alpha=\alpha', \tag{3.9b}$$

$$d/y=2-\alpha=\gamma+2\beta=\beta(\delta+1). \tag{3.9c}$$

The analysis which gives γ, γ', β, and δ is quite direct because it involves differentiating $\langle\sigma\rangle$. But the specific heat can only be found by integrating $\langle\sigma\rangle$ with respect to h. Even then there are no problems except when α is an integer. The interesting case is $\alpha=0$, which gives a singularity of the form

$$C_B(\epsilon, h=0) = -A \log|\epsilon| +B \quad \text{for } \epsilon>0$$

$$= -A' \log|\epsilon| +B' \quad \text{for } \epsilon<0. \tag{3.10}$$

This analysis indicates that the same coefficient multiplies the logarithm when $\epsilon>0$ and $\epsilon<0$:

$$A = A' \quad \text{for } \alpha=0. \tag{3.11}$$

Equation (3.11) is another conclusion drawn from the scaling laws which is subject to experimental verification.

TABLE IV. Check of scaling law equalities for Ising model. The scaling laws predict that, for a given transition, all the numbers listed in the table (except for Δ and y) should be the same.

	$2-\alpha$	$2-\alpha'$	$d\nu$	$d\nu'$	$d\gamma/(2-\eta)$	$\gamma+2\beta$	$\gamma'+2\beta$	$\beta(\delta+1)$	y	$\Delta=2x/y$
Two-dimensional Ising model	2	2	2	2	2	2	2	2	1	3.75
Three-dimensional Ising model	1.87 ± 0.12	1.93+0.04, −0.16	1.93 ± 0.01	?	1.933 ± 0.008	1.87 ± 0.01	1.94 ± 0.05	1.93 ± 0.05	1.55 ± 0.01	3.22 ± 0.02

C. Correlation Function Results

The next object is the spin–spin correlation function

$$g(\mathbf{r}, \mathbf{r}') = g(R, \epsilon, h) = \langle [\sigma_\mathbf{r} - \langle \sigma \rangle][\sigma_{\mathbf{r}'} - \langle \sigma \rangle] \rangle, \quad (3.12)$$

where R is the distance between the points in question, $R = |\mathbf{r} - \mathbf{r}'|/a_0$. We can equally well write a correlation function for the μ's defined by Eq. (3.4) which must be identical in structure to $g(R, \epsilon, h)$ except that the scales of length ϵ and h are changed

$$R \rightarrow R/L,$$

$$\epsilon \rightarrow \bar{\epsilon} = \epsilon L^y,$$

$$h \rightarrow \bar{h} = hL^x. \quad (3.13)$$

It follows that

$$g(R, \epsilon, h) = L^{2(x-d)} \langle [\mu_\mathbf{a} - \langle \mu \rangle][\mu_\mathbf{a}' - \langle \mu \rangle] \rangle$$

$$= L^{2(x-d)} g(R/L, \epsilon L^y, hL^x)$$

so that $g(R, \epsilon, h)$ can turn out to be independent of L, only if it has the structure:

$$g(R, \epsilon, h) = |\epsilon|^{2(d-x)/y} \tilde{g}(R|\epsilon|^{1/y}, \epsilon/|h|^{y/x}) \quad (3.14)$$

for $R \gg 1$, $|\epsilon| \ll 1$ and $h \ll 1$.

Equation (3.14) gives the critical indices ν, ν', and η. It is immediately apparent that the $h=0$ coherence length must be proportional to $|\epsilon|^{-1/y}$. Hence[43]

$$y^{-1} = \nu = \nu' = (2-\alpha)/d. \quad (3.15)$$

The last critical index is η, defined by

$$g(R, \epsilon=0, h=0) \sim (R^{d-2+\eta})^{-1}.$$

Then (3.9) and (3.13) give

$$d\gamma/(2-\eta) = 2-\alpha. \quad (3.16)$$

To conclude, we notice that arguments almost identical to the ones which generated the form (3.14) for the spin correlation function may be invoked to describe correlations involving the variable $E_\mathbf{r}$, which is the energy per site in the neighborhood of $\mathbf{r}$. The results are that

$$\langle [E_\mathbf{r} - \langle E \rangle][E_{\mathbf{r}'} - \langle E \rangle] \rangle$$

$$= g_{EE}(\mathbf{r}, \mathbf{r}')$$

$$= |\epsilon|^{2(d-\nu)/\nu} \tilde{g}_{EE}(R|\epsilon|^{1/\nu}, \epsilon/|h|^{\nu/x}) \quad (3.17a)$$

and

$$\langle [E_\mathbf{r} - \langle E \rangle][\sigma_{\mathbf{r}'} - \langle \sigma \rangle] \rangle$$

$$= g_{\sigma E}(\mathbf{r}, \mathbf{r}')$$

$$= |\epsilon|^{(2d-x-\nu)/\nu} \tilde{g}_{\sigma E}(R|\epsilon|^{1/\nu}, \epsilon/|h|^{\nu/x}), \quad (3.17b)$$

where $\tilde{g}_{EE}$ and $\tilde{g}_{\sigma E}$ represent unknown functions.

D. Comparison of Ising Model Results with Scaling Law Conclusions

The simplest conclusion from the scaling law hypothesis is that the combinations of "experimental parameters" $2-\alpha$, $2-\alpha'$, $d\nu$, $d\nu'$, $d\gamma/(2-\eta)$, $\gamma+2\beta$, $\gamma'+2\beta$, and $\beta(\delta+1)$ are all just different ways of writing the same number, d/y. To check this against the known Ising model results, we have given in Table IV the values of all these supposedly equal quantities as given by the results of Table II. The errors quoted in these tabulations are numerical errors in the Ising model analysis. The close equality among these numbers in both the two-dimensional case and three-dimensional one serves to support the scaling law hypothesis.

In the last two columns of Table IV values of y and $\Delta = 2x/y$ derived from the previous seven columns are quoted. [We use Δ as our basic variable because several other authors (e.g., Domb and Hunter) also use it.] The value of y is determined by using $\nu = 1/y$. The value of Δ is derived from y from the scaling law relation

$$\Delta = 2d\nu - 2\beta \quad (3.18)$$

since ν and β are known quite accurately.

In the two-dimensional case, there are available several other checks of the scaling law results. First the specific heat singularity at $h=0$ is logarithmic in character $(\alpha = \alpha' = 0)$ so that one should expect the coefficients A and A' defined by (3.10) are equal. The Onsager solution[9] shows this to be true.

Also, the scaling laws predict the following forms for the correlation functions of the two-dimensional Ising model at $h=0$. From (3.13), (3.16), and (3.17) it follows that at $h=0$,

$$g(\mathbf{r}, \mathbf{r}') = |\epsilon|^{1/4} G(\epsilon R), \quad (3.18a)$$

$$g_{\sigma E}(\mathbf{r}, \mathbf{r}') = |\epsilon|^{1+1/8} G_{\sigma E}(\epsilon R), \quad (3.18b)$$

$$g_{EE}(\mathbf{r}, \mathbf{r}') = |\epsilon|^2 G_{EE}(\epsilon R). \quad (3.18c)$$

All three of these scaling law conclusions have been verified by actual calculations.[11,18]

In conclusion, there is excellent evidence for the correctness of the scaling laws for the two-dimensional Ising model. All the correlation functions and critical indices turn out to agree exactly with the scaling law hypotheses. In three dimensions, the critical indices agree quite closely with this hypothesis, but there are small discrepancies which appear to be outside of the statistical uncertainties in the indices. These discrepancies have caused Domb[32] to have some doubt about the exact validity of these scaling laws which are derived from considerations involving the correlation functions, namely the relations involving ν and η. Fisher[33] has expressed similar reservations and also has questioned whether the symmetry above and below T_c, e.g., $\gamma = \gamma'$, is exactly true.

E. Questions About Real Phase Transitions

Three questions about the scaling laws which the experimental evidence can answer, in principle, are considered in this section.

A. Are the scaling laws correct?

Experimental evaluation of the indices combined with a comparison like that of Table IV can disprove the scaling laws or it can be strong evidence in their favor.

B. Assuming that the scaling laws are correct, how many different phase transitions are there?

We started from the point of view that the details of the interaction do not matter near the critical point. But what is a detail and what is essential? The dimensionality certainly matters considerably. But, in the real, three-dimensional world would we say all ferromagnetic transitions are essentially similar? Are these in turn just like all liquid gas transitions? Measurements of critical indices and deductions of values of x and y can shed considerable light on this point.

C. What are the values of x and y? Are they simple numbers like 2.5 or $\pi/2$? If so, careful thinking might serve to predict them. Accurate experimental determinations of these numbers can serve as a useful guide to thinking about this difficult problem.

IV. MAGNETIC TRANSITIONS

A. Theoretical Models

In real magnetic materials the spins are coupled through the strong, short-range exchange interactions and the long-range magnetic dipolar interactions. For the low-temperature materials, such as dysprosium aluminum garnet (DAG) and some low-temperature salts, these dipole interactions are of the same size or larger than the exchange interactions.[44–46] In high-temperature materials the exchange interactions are much stronger; however, even a weak long-range

interaction may affect the delicate correlations which occur quite close to the critical point.

No theories have been developed up to this point which can treat the complexity of a real magnetic material. Instead, theory deals with over-simplified models.

Molecular Field Theory

The simplest model is the molecular field theory or Landau theory. We discussed this extensively in Sec. II, where we mentioned that this model gave $\gamma = 1$, $\beta = \frac{1}{2}$, $\delta = 3$, and a finite discontinuity in C_H at the critical temperature. This model is appropriate whenever the force has a very long-range. In particular, if there are z equally interacting spins, then according to Brout[3] the molecular field theory works whenever $|\epsilon| = (T - T_c)/T_c | \gg z^{-1}$. The dipole interaction does not have a long enough range so that one can be sure that the Landau theory is valid for purely dipolar forces.

Ising Model

In the Ising model, one includes only one component of the spin. This model might be a suitable representation for highly anisotropic materials in which the coupling of one component of the spin is much stronger than that of the other two components.

Heisenberg Model

The Heisenberg model of the ferromagnet is, in some sense, an opposite limit to the Ising model. Here one assumes that the Hamiltonian contains terms of the form $J\mathbf{S} \cdot \mathbf{S}'$, where $\mathbf{S}$ and $\mathbf{S}'$ are the spin operators for neighboring particles.

This assumption of complete isotropy is stronger than just taking the crystal to contain three easy axes of magnetization—as in a cubic crystal. The Heisenberg model implies that all directions in space are equivalent. The order parameter is then the magnetization vector. Since this is qualitatively different from the scalar order parameter of the Ising model, the Heisenberg model may show a critical behavior which is qualitatively different from that of the Ising model.

Of the critical indices we are reviewing, the only numerical result for the three-dimensional Heisenberg model is for the critical index γ which describes the divergence of the susceptibility just above T_c. Numerical calculations give[47] $\gamma = 1.43$ for spin $\frac{1}{2}$ and[48] $\gamma = 1.33$ or[49] 1.36 for infinite spin. The three-dimensional Ising model gives $\gamma = 1.250$. This difference between the two models appears to be larger than the numerical errors in the calculation.

Notice the apparent spin dependence of the Heisenberg model's γ. The possibility that a critical index depends upon a specific detail of the interaction such as the size of the spin is contrary to the assumptions of the scaling laws. Consequently, we must count this

small spin dependence as an argument against the scaling laws.

Antiferromagnets

An antiferromagnetic ordering consists of two interpenetrating sublattices of equal and opposite magnetization. In this case the order parameter, $p(r)$, is the magnetization on each sublattice. The conjugate variable, h, is a magnetic field which is positive on one sublattice and negative on the other. There is no way of producing such a field macroscopically in the laboratory.

In the nearest-neighbor Ising model we convert a ferromagnetic ordering into an antiferromagnetic ordering by changing the sign of the interaction constant, K. Since this transformation may be undone by changing the signs of all the spin variables on one sublattice there is an exact equality between the partition functions of the ferromagnetic and antiferromagnetic Ising models. Therefore, all the zero field ($h=0$) conclusions of the Ising model apply equally well to the ferromagnet and antiferromagnet.[50]

An antiferromagnetic ordering may also be produced in the Heisenberg model by changing the sign of the interaction constant. However, in this situation, there is no exact correspondence between the problems for different signs of the interaction constant except at infinite spin. However, if the details of the interaction do not matter, and if the value of the spin is one such detail, then the Heisenberg model antiferromagnet would have the same critical indices as the Heisenberg model ferromagnet.

Because of the antiparallel sublattices, direct dipole–dipole interactions are of much shorter effective range than in ferromagnets. Therefore, these long-range forces should be expected to have a much smaller qualitative effect upon the transition in the antiferromagnetic case.

B. Problems in Interpreting Experimental Data

Concept of Critical Region and Determination of T_c

In interpreting the data we are not particularly interested in the absolute temperature, but in $\epsilon = \Delta T/T_c = (T-T_c)/T_c$ near a critical point. The temperature difference ΔT can be measured much more accurately than T itself.

Theoretically one assumes that the thermodynamic functions approach a simple behavior, namely, a power of ϵ, as $\epsilon \rightarrow 0$. Thus the critical region is defined as the region where this behavior dominates. Since molecular field theory fails for $\epsilon \lesssim 1/z$, where z is the number of nearest neighbors, we obtain a rough estimate that the critical region is for $\epsilon \lesssim 10^{-1}$. In fact, we shall show that for magnetic materials the experimental evidence indicates critical regions beginning when $\epsilon \lesssim 10^{-2}$ to 10^{-1}. [Since T_c varies from 0.1° to

1400°K in the materials studied, the critical region is most conveniently discussed in terms of ϵ rather than $(T-T_c)$ above.] In principle, one can make cross checks by comparing for example the regions in which the specific heat and the susceptibility seem to show critical behavior. In practice, there is rarely enough data on the same material to be confident that the various thermodynamic functions settle down to their critical behavior at the same ϵ.

A major experimental uncertainty is in the relative location of T_c itself. In specific heat measurements, a rounded peak is often observed, making the precise location of T_c uncertain (see Table IX). In resonance experiments one sometimes finds a small temperature region where both para- and antiferromagnetic lines exist (in external field) and overlap.[51,52] Measurements in applied field require extrapolation to zero field to fix T_c. Noakes, Tornberg, and Arrott[53] have taken some of this uncertainty into account by assuming a power-law temperature dependence and then fitting to the best value of T_c as well as the critical exponent. However, it would be most desirable to determine T_c independently of the above data, or at least through comparison of two critical quantities, such as specific heat and susceptibility.

An example illustrates how the choice of critical region and T_c are interdependent and affect the evaluation of critical indices: Heller[54] plots the cube of magnetization in MnF_2 vs the temperature. A linear relationship is found for $7 \times 10^{-5} < |\epsilon| < 8 \times 10^{-2}$, and this straight line is extrapolated to zero to give $T_c = 67.336 \pm 0.003°K$. Using his published data, however, we plot the *square* of magnetization vs. temperature and find that a straight line also fits here for $|\epsilon| < 10^{-3}$. Extrapolation gives $T_c = 67.343 \pm 0.004°K$. Consequently if we assume that the critical region is for $|\epsilon| \lesssim 10^{-1}$ we are forced to conclude that the cubic law is very nearly correct; if we assume that the critical region only includes $|\epsilon| \lesssim 10^{-3}$ then the data equally well permit the square and cube laws.

Domains

Ferromagnets and imperfect crystals of antiferromagnetic material have a tendency to break up into domains. The domain walls serve to break up the long-range correlations so essential to critical behavior. Hence, if one is to compare idealized theories (like the Heisenberg or Ising models) with experiments it is essential that the domains be larger than the theoretical coherence length. If this is not true there will be a rounding of the transition which will be very difficult to interpret.

Changes in Lattice Constants

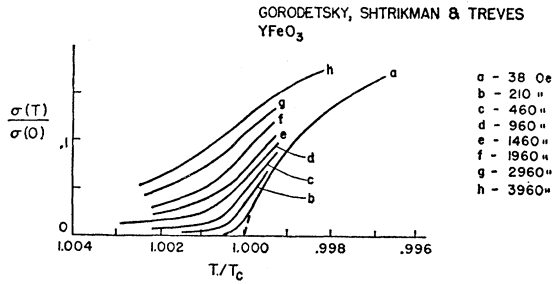The interaction constants which describe the coupling between spins depend upon the lattice parameters.

GORODETSKY, SHTRIKMAN & TREVES
YFeO₃

FIG. 3. Magnetization vs temperature of single-crystal YFeO₃ with the applied magnetic field as a parameter. The broken line is the magnetization extrapolated to $H=0$.

Since the internal energy of the lattice depends relatively strongly upon $T-T_c$ and T_c depends upon the lattice constants, it may be energetically favorable for the lattice constants to change near T_c. This effect should be included in the analysis of precise data.[54] In crude terms this is equivalent to say that $\epsilon=(T-T_c(T))/T_c$, i.e., for each temperature in the critical region we need a different T_c in order to look for a power law to compare with a theory which has fixed lattice constants.

This connection between critical effects and lattice size and shape can in some cases make the transition first order.[55] Consequently, it is necessary, in every case, to be convinced either that the transition is indeed second order or that the latent heat in a first-order transition is too small to change the effects under study.

C. Experimental Results

Susceptibility

The experiments are of two kinds:

(1) An experimental mapping of the M-H-T surface, such as reported by Gorodetsky, Shtrikman, and Treves[30] for the weak ferromagnet YFeO₃. Their curves are shown in Fig. 3. From these data one can obtain the spontaneous magnetization, M vs H at T_c, and the susceptibility above and below T_c. To find T_c and the spontaneous magnetization one must extrapolate such data to $H=0$. To find the susceptibility below T_c one must subtract the spontaneous magnetization from the measured magnetization, which can introduce considerable uncertainty.

(2) Neutron scattering measures a time-dependent spin–spin correlation function from which one can deduce the correlation length and the susceptibility.

The experimental susceptibility data are summarized in Table V.[56–59] Except for YFeO₃ all the data are for $T>T_c$. The effective spin is listed in each case, but one cannot tell from these data whether the Heisenberg model behavior of larger γ for smaller spin is followed. The effects of single crystal versus polycrystal are

more evident. Gadolinium is anisotropic, and Graham[60] has pointed out that for a single-crystal susceptibility measurements along the easy axis and along a hard axis show different behavior. Thus Develey's recent $\gamma\approx1.16$ for polycrystalline gadolinium is not surprising.[57] Possibly the $\gamma\approx1.21$ for polycrystalline cobalt has a similar explanation.[61] Iron and nickel each have three easy axes of magnetization and polycrystalline samples show the typical $\gamma\approx\frac{4}{3}$.

The recent experiment by Noakes, Tornberg, and Arrott shows that in iron the susceptibility and hence the long-range correlations are not altered by impurities.[53] The one value for $T<T_c$, namely $\gamma'\approx0.7$ in YFeO₃,[30] violates the scaling law prediction $\gamma=\gamma'$.

In experiments of Miedema, Van Kempen, and Huiskamp[45] on the low-temperature salt CuK₂Cl₄·2H₂O, they also measured its specific heat (see Table IX). Our analysis indicates the specific heat settles down to its critical behavior for $\epsilon<10^{-1}$ whereas the susceptibility has settled down for $\epsilon<3\times10^{-1}$. Comparative data such as this should always be an objective of a critical phenomena experiment, for it helps establish where the critical region begins. In this case it appears that the critical region is approximately the same for these two thermodynamic functions.

Kouvel[62] has used M vs H and T data to construct a very direct check of the scaling laws. According to Eq. (3.7), for a given material the magnetization obeys the relation

$$M/\epsilon^\beta=f(H/\epsilon^{\beta\delta}),\qquad(4.1)$$

where $f(H/\epsilon^{\beta\delta})$ is an unknown function. From (4.1) we conclude that if we knew M as a function of H for one value of ϵ and if we knew β then we could predict M vs H for any other value of ϵ. [Actually this is not quite true because $f(H/\epsilon^{\beta\delta})$ can have two different forms, one for $\epsilon>0$ and the other for $\epsilon<0$. But as long as we remain above T_c, the scaling laws predict that one measurement of M vs H would suffice to tell everything.]

Kouvel used the data of Weiss and Forrer[58] for Ni and his own data for CrO₂ [62] to construct a direct check of Eq. (4.1). He plotted M/ϵ^β as a function of $H/\epsilon^{\beta\delta}$ for different values of ϵ as indicated in Fig. 4. If Eq. (4.1) is correct this plot should give a simple curve, independent of the value of ϵ. The figure indicates that the points do fall on one curve. This then serves as a direct and convincing check of the scaling laws.

This analysis provides values of β and $\beta\delta$ which are different for the two materials. In particular, we have

$$\beta=0.42\qquad\beta\delta=1.76\qquad\text{for Ni}$$

$$\beta=0.33\qquad\beta\delta=1.91\qquad\text{for CrO}_2.\qquad(4.2)$$

Equation (4.1) indicates that the critical index γ is given in terms of these as

$$\gamma=\beta(\delta-1).\qquad(4.3)$$

TABLE V. Ferromagnetic susceptibility $T > T_c$.

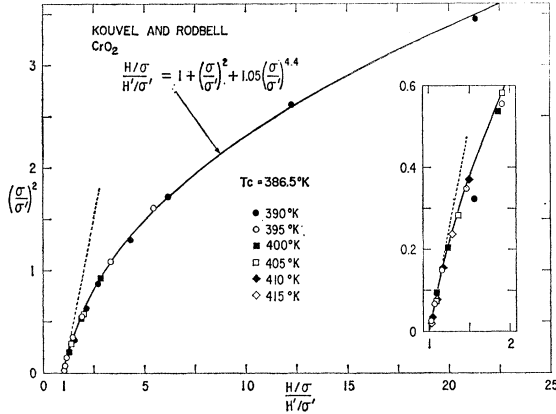| Material	Experimenters	Ref.	Method	T_c (°K)	$\epsilon = \Delta T/T_c$ Range for fit	γ	Effective spin	Comments
Iron	Arajs, Colvin	56	Field gradient force technique	1044.0	10^{-3}–4×10^{-2}	1.33	1.1	
	Noakes, Tornberg, Arrott	53	Induction	1044.0	5×10^{-5}–1.5×10^{-2}	1.333 ± 0.015		$\gamma=1.32$–1.35 for alloys less than 2.4%
	Develey	57	Moving balance	1041.8	2×10^{-3}–3×10^{-2}	1.33 ± 0.03		
Nickel	Weiss, Forrer	58	Magnetocaloric effect	627.2	4×10^{-3}–3×10^{-2}	1.35 ± 0.02	0.3	
	Arajs	59	Field gradient force technique	626.5	2×10^{-3}–2×10^{-2}	1.29 ± 0.03		
	Develey	57	Moving balance	631.0	5×10^{-3}–3×10^{-2}	1.32 ± 0.02		
Gadolinium	Graham	60	Fluxmeter	292.5	3×10^{-3}–5×10^{-2}	1.33	7/2	Single crystal contains some Gd_2O_3
	Develey	57	Moving balance	292.85	2×10^{-3}–5×10^{-2}	1.16 ± 0.02		Not single crystal
Cobalt	Colvin, Arajs	61	Field gradient force technique	1388.2	7×10^{-4}–10^{-2}	1.21 ± 0.04	0.85	Not single crystal
$CuK_2Cl_4\cdot2\ H_2O$ $Cu(NH_4)_2Cl_4\cdot2\ H_2O$	Miedema, VanKempen, Huiskamp	45	ac bridge and ballistic galvanometer	0.88 0.70	3×10^{-2}–3×10^{-1} 4×10^{-2}–4×10^{-1}	1.36 1.37	1/2	
$YFeO_3$	Gorodetsky, Shtrikman, Treves	30	Vibrating sample magnetometer	643	2×10^{-4}–3×10^{-3}	1.33 ± 0.04	1.1	$\gamma'=0.7\pm0.1$
CrO_2	Kouvel, Rodbell	62		386.5	2×10^{-2}–2×10^{-1}	1.6 ± 0.05	1	
Value used for scaling law analysis						1.33 ± 0.03		
Molecular field theory						1.0		
3-dimensional Ising model						1.250 ± 0.001		
3-dimensional Heisenberg model						1.33 ± 0.05/spin (Ref. 63)		

FIG. 4. Magnetization vs field for CrO_2. In our notation, $\sigma = M$, $\sigma' \sim \epsilon^\beta$, $H'/\sigma' \sim \epsilon^\gamma = \epsilon^{\beta(\delta-1)}$. Points for different ϵ fall on the same curve, which verifies the scaling law prediction, Eq. (4.1).

The resulting values of γ have been inserted in Table V. Also the index δ, defined by

$$M \sim H^{1/\delta} \quad \text{at} \quad T = T_c$$

can be identified with the quantity δ defined by Eq. (4.1). Therefore Kouvel's analysis gives the values of δ. These have been inserted in Table VIII.

If we assume the scaling law conclusion that (4.1) is equally correct for $\epsilon > 0$ and $\epsilon < 0$ with the same value of β and δ but a different f, then we find that

$$M \sim (-\epsilon)^\beta$$

for $\epsilon < 0$ and $H = 0$. This would permit us to identify the quantity, β, determined by Kouvel's analysis [see Eq. (4.2)] with the critical index, β, which defines the behavior of the magnetization for $T < T_c$. However, Kouvel provides no experimental evidence for (or against) this extrapolation into the region $T < T_c$.

Neutron Scattering

Magnetic systems have an anomalously large cross section for neutron scattering near their critical temperature. Van Hove[64] has shown that this is due to the large fluctuations in magnetization near T_c. An excellent review of this subject has been written by DeGennes.[65]

Passel, Blinowski, Brun, and Nielsen[66] have measured the neutron scattering cross section for iron. Their experiment can be interpreted in terms of the formula for the cross section

$$\frac{d}{dE}\frac{d\sigma}{d\Omega} \sim \int dt \exp(-i\omega t) \sum_R \langle S_0 S_R(t) \rangle \exp(i\mathbf{q} \cdot \mathbf{R}).$$

$$(4.4)$$

Here E is the scattered neutron energy, q and ω are the momentum and energy transferred from the neutron to the magnetic material, R is a lattice site, and S is a spin operator. Van Hove[64] has described

the time dependence of the correlation function by expressing the decay of a fluctuation in the magnetization by a diffusion equation with diffusion coefficient Λ.

This implies that the correlation function in Eq. (4.4) decays in time according to

$$\sum_R \exp(i\mathbf{q} \cdot \mathbf{R}) \langle S_0 S_R(t) \rangle$$

$$= \sum_R \exp(i\mathbf{q} \cdot \mathbf{R} - \Lambda q^2 t) \langle S_0 S_R \rangle. \quad (4.5)$$

Thus, the cross section in (4.4) can be expressed in terms of the static correlation function $\langle S_0 S_R \rangle$. According to the scaling laws, at zero magnetic field,

$$\langle S_0 S_R \rangle = G(R/\xi)/R^{1+\eta}, \quad (4.6)$$

where ξ is the coherence length. This is supposed to depend upon temperature as

$$\xi \sim \epsilon^{-\nu}.$$

The dependence of the correlation function upon $(T - T_c)$ is supposed to be hidden in the dependence of the unknown function, G, upon R/ξ.

In analyzing the experiments, it is convenient to guess[16] the form of G as

$$G(R/\xi) = A \exp(-R/\xi) \quad \text{for } T > T_c, \quad (4.7)$$

where A depends only very weakly upon ϵ. [When $\eta = 0$, this gives the Ornstein–Zernike[67] result for the correlation function

$$\langle S_0 S_R \rangle = A(e^{-R/\xi}/R).] \quad (4.8)$$

If we put together the results (4.5), (4.6), and (4.7) we find the differential cross section as

$$\frac{d\sigma}{d\Omega} \sim A(T) \int d\omega \frac{\Lambda_q^2}{(\Lambda^2 q^4 + \omega^2)(\xi^{-2} + q^2)^{1-1/2\eta}}. \quad (4.9)$$

Passel, Blinowski, Brun, and Nielsen obtained the parameters $A(T)$, Λ, and $\xi(T)$ by comparing their data with $d\sigma/d\Omega$ for various choices of η. For $\eta = 0$, the result is $\nu = 0.64 \pm 0.02$ in $7 \times 10^{-3} < \epsilon < 6 \times 10^{-2}$. For $\eta = 0.15$, the result is $\nu = 0.64 \pm 0.02$ in $4 \times 10^{-3} < \epsilon < 6 \times 10^{-2}$. So $\eta \neq 0$ fits the data better for smaller ϵ. However, experimental uncertainty for $\epsilon < 10^{-2}$ precludes drawing any conclusions about the value of η.

Above T_c, the susceptibility is given in terms of the spin–spin correlation function by the relation

$$\chi \sim \sum_R \langle S_0 S_R \rangle$$

From (4.6) and (4.7) it follows that

$$\chi \sim A(T)\xi^{2-\eta}. \quad (4.10)$$

If we express the coherence length $\xi \sim \epsilon^{-\nu}$, and if ϵ is small enough so that $A = \text{constant}$, then $\chi \sim \epsilon^{-\gamma}$ implies $\gamma = (2 - \eta)\nu$. Unfortunately, this experiment did not extend to small enough values of ϵ for A to be a constant

TABLE VI. Correlation length $T > T_c$.

Material	Experimenters	Ref.	Method	T_c (°K)	$\epsilon = \Delta T/T_c$ Range for fit	ν	Comments
Iron	Passell, Blinowski, Brun, Nielsen	66	Neutron scattering	1044.0	5×10^{-3}–6×10^{-2}	0.64 ± 0.02	$\eta=0.07\pm0.07$
Cr_2O_3 α-Fe_2O_3	Riste, Wanic	68	Neutron scattering	310.0 998.0	10^{-2}–5×10^{-2} 5×10^{-3}–7×10^{-2}	0.67 ± 0.03 0.63 ± 0.04	Antiferromagnets
$KMnF_3$	Cooper, Nathans	69	Neutron scattering	88.06 ± 0.02	2×10^{-3}–10^{-1}	0.67 ± 0.04[a]	Antiferromagnet
Value used for scaling law analysis						0.65 ± 0.03	$\eta=0.07\pm0.07$
Molecular field theory						0.5	$\eta=0$
3-dimensional Ising model						0.643 ± 0.003	$\eta=0.056\pm0.008$

[a] This paper reports the temperature dependence of the staggered susceptibility, which is simply related to the square of the correlation length, as discussed in our text for iron.

$[A\sim(r_1^2)^{-1}$ in Ref. 66], so we cannot take $\gamma=(2-\eta)\nu$ here. Nevertheless one can plot $A\xi^{2-\eta}$ vs ϵ and obtain an approximate fit by $\epsilon^{-\gamma}$, to obtain $\gamma=1.30$. This agrees with γ for iron as listed in Table V.

In antiferromagnets, $\langle S_0 S_R \rangle$ is defined with respect to a sublattice, and again we write $\xi \sim \epsilon^{-\nu}$. Values of ν and η for three antiferromagnets, iron, and theoretical models are listed in Table VI.[66,68,69]

Magnetization

The most accurate measurements of magnetization, indeed the only ones possible for antiferromagnets, are measurements of internal fields, e.g., at nuclei through NMR or the Mössbauer effect. Can we be sure that the hyperfine field H_n is linearly related to the bulk or sublattice magnetization? The data we quote assume this, but it is not at all obvious in the study of hyperfine interactions.[70] Experimental evidence indicates nonlinearity between magnetization and hyperfine field in some cases. In iron, the Mössbauer measurement of Preston, Hanna, and Heberle[71] agrees with the NMR result (which is at low temperatures only) on relative H_n variation with temperature, but is in slight disagreement with the bulk magnetization measurement. Many authors find that *impurity* hyperfine fields are not directly proportional to bulk magnetization.[72] Callen, Hone, and Heeger[73] and more recently Hone, Callen, and Walker[74] deduce theoretically nonlinear relationships between impurity and host *magnetizations*. On the other hand, both experimental and theoretical results point to a linear relationship between H_n and M as $T \to T_c$, even for impurities, thus supporting the usefulness of hyperfine field measurement in the study of critical phenomena.

The experimental results are listed in Table VII. For the ferromagnetic materials they show $\beta \approx \frac{1}{3}$ for relatively high values of $-\epsilon$, i.e., $3\times10^{-3} \lesssim -\epsilon \lesssim 10^{-1}$. However, for small values of ϵ there are two experiments, on Ni^{29} and $YFeO_3$[30] which indicate higher values of β, namely $\beta \approx \frac{1}{2}$. This apparent change in index at $(-\epsilon) \sim 3\times10^{-3}$ is perplexing. A theory due to Callen and Callen[75] predicts this kind of behavior, but one wonders what it would predict for other critical quantities, e.g., susceptibility and specific heat. Recent preliminary data of Arrott[75a] indicate $\beta \approx \frac{3}{8}$ for nickel in the same temperature region in which Ref. 29 reported $\beta = \frac{1}{2}$.

We suggest tentatively that this change in the value of β might be caused by the dipole forces in the ferromagnet. These dipole forces are weak in comparison with the exchange forces so that they should not be expected to modify the thermodynamic functions very much under usual circumstances. However, very near T_c, there are very delicate and long-range correlations which might be affected materially by these dipole fields. Since the dipole force is long-range, it might be expected to produce qualitatively different critical behavior from that produced by the short-range exchange forces. Hence, as the critical point, is approached, a change in β might occur at some value of ϵ for which the dipole forces just become important.

To estimate this critical value of $(-\epsilon)$, assume that, because large regions of spins fluctuate in their magnetization, there are fluctuations in the magnetization just about as big as the average magnetization. This would imply that there are fluctuations in the magnetic field, δB, which are of the order of the average magnetization:

$$\delta B \sim \langle M \rangle. \tag{4.11}$$

Now let us try to estimate how much damage these fluctuations in B can do. When can they appreciably modify the results that we would get from a theory in which the magnetic forces were left out? To do this compare the spontaneous magnetization, which is given by

$$M/M_0 \sim (-\epsilon)^\beta \qquad \text{at } B=0 \tag{4.12}$$

TABLE VII. Spontaneous magnetization.

Material	Experimenters	Ref.	Method	T_c (°K)	$\epsilon = |\Delta T|/T_c$ Range for fit	β	Comments
Antiferromagnets							
MnF₂	Heller, Benedek	51	NMR on F[19]	67.336±0.003	8×10^{-5}–2×10^{-2}	0.335±0.01	
CuCl₂·2H₂O	Poulis, Hardeman	76	NMR, Protons	4.337±0.003	5×10^{-4}–10^{-2} 10^{-2}–10^{-1}	0.18±0.07 0.29±0.03	
CoCl₂·6H₂O	Sawatzky, Bloom	52	NMR, Protons	2.275	10^{-2}–10^{-1}	0.15±0.05	
	Van der Lugt, Poulis	77	NMR, Protons	2.275	5×10^{-2}–2×10^{-1}	0.23±0.02	
KMnF₃	Cooper, Nathans	69	Neutron scattering	88.06±0.02	10^{-2}–10^{-1}	0.33	
Ferromagnets							
Iron	Preston, Hanna, Heberle	71	Mössbauer Fe[57]	1042.0±0.3	2×10^{-3}–10^{-1}	0.34±0.02	Only four data points in this region
Nickel	Potter	78	Magnetocaloric effect	1035.0±2.0	4×10^{-3}–2×10^{-1}	0.36±0.08	Large uncertainty possible in T_c
	Howard, Dunlap, Dash	29	Mössbauer Fe[57]	629.4	5×10^{-4}–10^{-2} 10^{-2}–1.6×10^{-1}	0.51±0.04 0.33±0.03	
EuS	Heller, Benedek	79	NMR, Eu[153]	16.50±0.03	10^{-2}–10^{-1}	0.33±0.015	
YFeO₃	Gorodetsky, Shtrikman, Treves	30	Vibrating sample magnetometer	643	2×10^{-4}–3×10^{-3}	0.55±0.04	
	Eibschutz, Shtrikman, Treves	80	Mössbauer Fe[57]	640	10^{-2}–3×10^{-1}	0.354±0.005	$\beta=0.348\pm0.005$ is average for fourteen rare-earth orthoferrites
CrBr₃	Senturia, Benedek	81	NMR, Br[79], Br[81]	32.56±0.015	7×10^{-3}–5×10^{-2}	0.365±0.015	
Value used for scaling law analysis						0.33±0.03	
Molecular field theory						0.5	
3-dimensional Ising model						0.313±0.004	

TABLE VIII. M vs H at T_c.

Material	Experimenters	Ref.	Method	T_c (°K)	δ	Comments
Nickel	Weiss, Forrer	58	Magnetocaloric effect	627.2	4.2±0.1[a]	
Gadolinium	Graham	60	Fluxmeter	292.5	4.0±0.1	
YFeO$_3$	Gorodetsky, Shtrikman, Treves	30	Vibrating sample magnetometer	643.0	2.8±0.3	Weak ferromagnet
CrO$_2$	Kouvel, Rodbell	62		386.5	5.75	
Value used for scaling law analysis					4.1±0.1	
Molecular field theory					3.0	
3-dimensional Ising model					5.2±0.15	

[a] Recent preliminary data of Arrott indicate $\delta \approx 4.7$ for nickel. This work was reported to the Twelfth Annual Conference on Magnetism and Magnetic Materials, Washington, D. C., November 1966.

with the induced magnetization

$$M/M_0 \sim (\mu B/KT_c)^{1/\delta} \quad \text{at } \epsilon = 0, \qquad (4.13)$$

where M_0 is the zero temperature magnetization and μ_B is the Bohr magneton. From (4.11) and 4(.13), we would guess that the fluctuations in B would modify the magnetization by an amount of the order

$$(\delta M) \sim (\mu M/KT_c)^{1/\delta} M_0. \qquad (4.14)$$

If this modification is negligible in comparison with the underlying magnetization given by (4.12), then we can neglect the long-range forces. This condition is

$$(\mu M/KT_c)^{1/\delta} \ll (-\epsilon)^\beta.$$

We substitute for M by using (4.12) and find

$$(-\epsilon) \gg (\mu M_0/KT_c)^{1/\beta(\delta-1)} \qquad (4.15)$$

as our condition for neglecting the dipole forces.

To evaluate this condition we choose $\beta = \frac{1}{3}$, $\delta = 4.2$, $M_0 = \mu \times (\text{density}) = \mu \times (10^{23} \text{ atoms/cm}^3)$, $T_c = 600°K$ and find that the condition (4.15) has become

$$(-\epsilon) \gg 10^{-2} \quad \text{for Ni.}$$

From this point of view, it is not surprising that Ni should have a change in β at this point.

This calculation suggests that the $\beta \approx \frac{1}{2}$ observed in YFeO$_3$ and Ni and the $\gamma' \approx 0.7$ in YFeO$_3$ might be characteristic of an effect of long-range dipole forces rather than the theoretically simpler short-range forces. If so, perhaps specific heat and susceptibility data below T_c should also approach molecular field values. The only applicable datum, however, is $\gamma' \approx 0.7$ in YFeO$_3$.[30]

The experimental data for iron are not sufficiently clear cut to support or deny the calculation just made. Preston, Hanna, and Heberle's result for β is based on a very small number of data points[77a] but indicates $\beta \approx \frac{1}{3}$ for $-\epsilon > 2 \times 10^{-3}$.[71] Potter's data may be interpreted either as fitting one power law with a large error or as gradually changing its β, with β increasing as $\epsilon \to 0$.[78] There is clearly a need for further investigation in this area.

Of the antiferromagnets listed in Table VII, only MnF$_2$ has been carefully investigated for $\epsilon < 10^{-2}$.[51] In several experiments NMR lines have been observed at the same temperature corresponding to the antiferromagnetic and paramagnetic state simultaneously.[51,52] This may be due to nonuniform T_c, or possibly to fluctuations in magnetization of sufficiently large space and time extent.

A clear-cut picture does not emerge from these measurements of β. However, on the basis of this rather scanty evidence we might propose that there are three separate behaviors here:

(a) When dipole forces are not important, $\beta \approx \frac{1}{3}$ in both ferromagnets and antiferromagnets. Hence, for our analysis of experiments which do not seem to be affected by these long-range forces we use $\beta = 0.33 \pm 0.03$.

(b) In high-temperature ferromagnets very close to T_c, β seems to be about $\frac{1}{2}$. This might be caused by the dipole forces—which are unimportant far from T_c—but which might produce important corrections very near T_c.

(c) The experiments on CuCl$_2$·2 H$_2$O[76] and CoCl$_2$· 6 H$_2$O[52,77] yield still other values for β, suggesting that these materials are more complicated than can be accounted for by our simple picture. These are low-temperature antiferromagnets where dipole forces are comparable in magnitude with exchange forces.

M vs H at T_c

Molecular field theory predicts $M \sim H^{1/3}$ at T_c. More generally we write $M \sim H^{1/\delta}$. Table VIII lists four experimental values of δ. It is tempting to try to get values of δ for nickel,[59] iron,[56] and cobalt[61] from the data of Arajs and Colvin, since they also publish M vs H vs T, but in fact the magnetic fields they used are too small for this purpose. To find δ, one needs ϵ to be negligible. However, a comparison of Eqs. (4.12) and (4.13) indicates that ϵ can only be neglected if

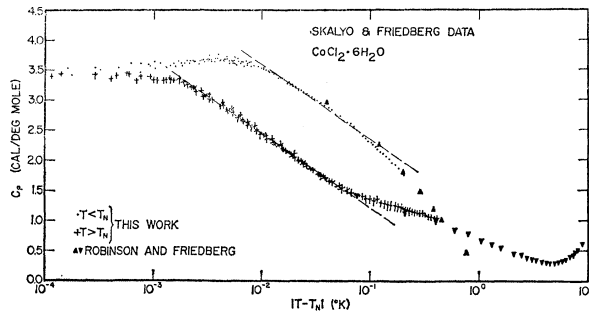$$|\epsilon|^\beta \ll (\mu H/KT_c)^{1/\delta}. \qquad (4.16)$$

Fig. 5. Specific heat of $CoCl_2 \cdot 6 H_2O$. The peaks round off for $\epsilon \approx 5 \times 10^{-3}$.

However, the uncertainty in T_c precludes satisfying Eq. (4.16). This uncertainty arises in the case of Arajs and Colvin, because they had to extrapolate from $H \neq 0$ to determine T_c. Thus their T_c for cobalt can easily be in error by $\pm 0.05°K$. Assuming $\delta \approx 4$ and $\beta \approx \frac{1}{3}$, the fields H_i (applied field corrected for demagnetizing effects) are not large enough to allow a determination of δ.

Specific Heat

The specific heat results are perhaps the most difficult critical data to categorize and understand In the two-dimensional Ising model, the specific heat behaves as

$$C_H = - A \log | \epsilon | + B \qquad \text{for } T > T_c$$
$$= - A' \log | \epsilon | + B' \qquad \text{for } T < T_c, \quad (4.17)$$

with $A = A'$ and $B = B'$. In molecular field theory, there is a discontinuity in the specific heat. This corresponds to the result (4.17) in the special case $A = A' = 0$, $B \neq B'$. However, in the analysis of the three-dimensional Ising model, it has been suggested[16] that the specific heat diverges more strongly than indicated in (4.17), in fact that

$$C_H \sim a \epsilon^{-\alpha} + b \qquad \text{for } T > T_c$$
$$\sim a' | \epsilon |^{-\alpha'} + b' \qquad \text{for } T < T_c, \quad (4.18)$$

with $\alpha \sim \alpha' \sim 0.1$. In writing Eq. (4.18), we have included terms in b and b' which are asymptotically much smaller than the divergent terms in (4.18). Hence they would be left out of the numerical analysis. However, there is no theoretical reason why these constant terms should not arise as slightly less divergent terms in the specific heat. Finally, there have been suggestions[82] that the specific heat might be less singular than indicated in (4.17) or (4.18). This behavior could arise, for example, if $b = b'$ in Eq. (4.18) and α and α' were both negative. Then C_H would show neither an infinity nor a discontinuity, but just a cusp equivalent to a third order phase transition.[83]

We would like to deduce the α's from the experimental data. This is difficult because what we wish to see is a weakly singular term above the background of b and b'. Given a bit of scatter in the experimental points, it becomes possible to make the three-parameter (a, b, α) fit indicated in Eq. (4.18) with a whole range of α's. A fit of the form (4.17) emerges as just a special case of the fit (4.18) since

$$\lim_{\alpha \to 0} (A/\alpha) [\epsilon^{-\alpha} - 1] + B = - A \log \epsilon + B. \quad (4.19)$$

It is hard enough to take data for, say $T > T_c$ and try to make a three-parameter fit as indicated in Eq. (4.18). But, actually the problem is much harder. One is supposed to reject all data for large values of $| \epsilon |$ since these data are "not in the critical region." This choice of which data are to be thrown out will influence considerably the range of α's which will fit the experiment. Also, there is often (see Fig. 5) some rounding of the peaks in the specific heat—which one might guess is due to imperfections in the crystals. It is tempting to say that this is the cause of the rounding and reject the data in the rounded region. But, if this is done, one more unknown parameter enters the problem: T_c. Clearly, if there is a broadening of the specific heat maximum, we cannot use the position of the peak to determine T_c with high precision.

Despite all this, it is possible to make some statements about α and α'. Consider, for example, the data of Skalyo and Friedberg[84] shown in Fig. 5. This plotting indicates that we can get a simple result if we reject all data for $| \epsilon | > 4 \times 10^{-2}$ as "not critical," and all data for $C_P > 3.3$ cal/(deg-mole) as "produced by crystalline imperfections." Then the figure indicates that the remaining data—which extends over only about one decade in ϵ—fit a logarithmic singularity. However, these remaining data also can be fitted by Eq. (4.18) with all values of α in the range

$$0 \leq \alpha' \lesssim 0.11$$
$$0 \leq \alpha \lesssim 0.19.$$

In Skalyo and Friedberg's data one is somewhat free to choose T_c because of the rounding off in the specific heat curve. Thus they chose $T_c = 2.289°K$ because it gave $A'/A = 1$. We find $T_c = 2.288°K$ gives an equally good logarithmic fit but yields $A'/A \approx 0.8$. Thus we see that A'/A is extremely sensitive to our choice of T_c.

Our range of α's becomes even larger if we consider data[85] like that in Fig. 6. If we say that the critical region is $| \epsilon | < 10^{-1}$, we are forced to fit the data with a large power of $(T - T_c)$. In particular, we find $\alpha \approx 0.6$ for Co $K_2(SO_4) \cdot 6 H_2O$ and $\alpha \approx 0.7$ for Co $Cs_3 Cl_5$. However, choosing the critical region to be $| \epsilon | < 2 \times 10^{-2}$ we can fit the data for α's between zero and roughly 0.6. In short, we cannot distinguish between $\alpha = 0$ and $\alpha = 0.6$ from these data.

Our experience is that at least two decades of data are desirable to establish the specific heat behavior. We also find that in order to fit data to a single logarithm or low power law we must often limit the critical region to $\epsilon \lesssim 10^{-2}$. This often leaves only one decade of critical data.

The rounding of the specific heat peak still may indicate that the specific heat is not a divergent function.

The experiment of Teaney[86] on the specific heat of MnF_2 best allows one to make a definite statement about α and α', for he obtained data over more than two decades and down to $\epsilon = 2 \times 10^{-4}$ with no rounding of the peak.

Figure 7 shows the specific heat of MnF_2 plotted on semilog paper. Both the logarithm and power law seem satisfactory over substantially the same temperature range. Figure 8 shows the effects of introducing various b' into the data. Sublattice magnetization data for MnF_2[87] indicates that $\epsilon \lesssim 2 \times 10^{-2}$ specifies the critical region. If we use this cutoff to determine the range of α allowed in the three-parameter fit, then $0 \lesssim \alpha' \lesssim 0.18$. Similarly, for iron[88] the susceptibility data above T_c indicates a critical region of $\epsilon \lesssim 2 \times 10^{-2}$, leading to $0 \lesssim \alpha \lesssim 0.17$.

In Table IX are listed ranges for α and α' obtained from three parameter fits. In these cases critical data exist over a wide enough temperature interval to make such an analysis meaningful. There is a reasonable amount of data for which $\alpha \lesssim 0.16$. We use this value for the purposes of checking the scaling laws. But there are also considerable data which apparently do not fall into this category.

This table includes a column labeled A'/A which is found by taking the logarithmic fits to the data and finding the ratio of coefficients above and below T_c. In four of the five cases this ratio agrees with the
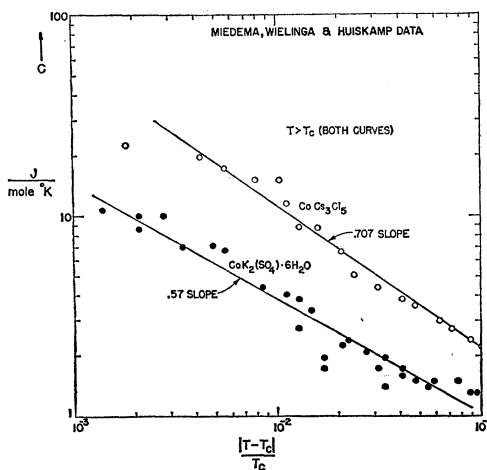
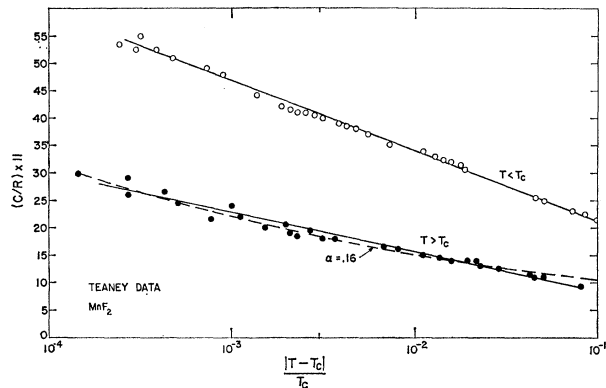FIG. 7. Specific heat of MnF_2 as measured by Teaney. The solid lines represent logarithmic fits. The dashed line is the power law $C \sim \epsilon^{-0.16}$.

scaling law conclusion $A'/A = 1$. However, for the best experiment, MnF_2,[86] this result fails. Either the specific heat is not logarithmic for MnF_2 or this conclusion drawn from the scaling laws is wrong.

Specific Heat in External Fields

The second-order phase transition in an antiferromagnet is not destroyed upon application of an external field, as it is in a ferromagnet. According to a theory by Fisher[94] the critical temperature is lowered as $T_c(H) = T_c(0) - aH^2$. Recent results for dysprosium aluminum garnet[95] agree with this prediction close to T_c. Data for $MnCl_2 \cdot 4\ H_2O$[96] indicate that the specific heat peak moves to lower T as H increases, but the peak also is broadened considerably, which makes the data difficult to interpret.

Comparison with Scaling Laws

Tables V–IX indicate the average values used in comparing the scaling law relations. Values which obviously contradict the chosen values are $\beta \approx \frac{1}{2}$ in nickel and $\beta \approx \frac{1}{2}$, $\gamma' \approx 0.7$, $\delta \approx 2.8$ in $YFeO_3$. This is a pattern of roughly molecular field theory behavior which might be explained by long-range forces which act in the presence of substantial spin alignment. For scaling law comparisons we neglect these data, but not because we consider them unreliable. The scaling laws are only applicable for short-range interactions, so that they might not apply to these data.

The comparisons are shown in Table X. Most of the data fit the pattern, although the column involving δ does not fit well. For antiferromagnets the scaling laws seem all right, upon very limited evidence, so definite conclusion cannot be drawn. For ferromagnets, the scaling laws relate a part of the data, but another part remains outside this framework. Further theoretical work on the effects of the long-range force might reconcile the apparent discrepancies.

FIG. 6. Examples of specific heat data which are apparently fit by relatively large power laws.

TABLE IX. Specific heat.[a]

Material	Experimenters	Ref.	T_c (°K)	$\epsilon = \lvert \Delta T \rvert / T_c$ Range for fit	α	α'	A'/A	Comments
Antiferromagnets								
MnF₂	Teaney	86	67.33±0.01	2×10^{-4}–5×10^{-2}	$\lesssim0.16$	$\lesssim0.18$	2.0	
CoCl₂·6 H₂O	Skalyo, Friedberg	84	2.289±0.002	10^{-3}–3×10^{-2} 5×10^{-3}–4×10^{-2}	$\lesssim0.11$	$\lesssim0.19$	1.0	Rounding of peak
MnCl₂·4 H₂O	Friedberg, Wasscher	89	1.622±0.005	10^{-2}–10^{-1}		$\lesssim0.14$		$T>T_c$, Logarithm fits data for 4×10^{-3}–2×10^{-2}
CuK₂(SO₄)₂·6 H₂O	Miedema, Wielinga, Huiskamp	85	0.193±0.001	10^{-2}–2×10^{-2}	$\lesssim0.6$			
CoCs₃Cl₆			0.52±0.01	4×10^{-3}–2×10^{-2} 4×10^{-3}–5×10^{-2}	$\lesssim0.7$	$\lesssim0.25$		Rounding of peak
RbMnF₃	Teaney, Moruzzi, Argyle	90	0.83±0.01	2×10^{-4}–5×10^{-2} 2×10^{-3}–2×10^{-2}	$\lesssim0.15$	$\lesssim0.15$	1.0	Rounding of peak
Ferromagnets								
Iron	Kraftmakher, Romashina	91	1043.0±1.0	2×10^{-3}–10^{-1} 3×10^{-3}–7×10^{-2}	$\lesssim0.17$	$\lesssim0.13$	1.0	
CuK₂Cl₄·2 H₂O	Miedema, Wielinga, Huiskamp	92	0.88±0.01	10^{-2}–10^{-1}	$\lesssim0.10$	$\lesssim0.17$	1.0	
Nickel	Kraftmakher	93	627.0	5×10^{-3}–8×10^{-2}				Data have considerable scatter. Logarithms with $A'/A \approx 1$ provide reasonable fit.
Value used for scaling law analysis					$\lesssim0.16$	$\lesssim0.16$		
Molecular field theory					0	0		Finite discontinuity
3-dimensional Ising model					$\lesssim0.2$	$\lesssim0.1$		

[a] Further information on magnetic specific heats may be found in Ref. 1, particularly the papers of Teaney and Yamamoto et al.

FIG. 8. Three-parameter |fits for $\frac{C}{R} - b'$ specific heat of MnF$_2$ for $T < T_N$. Dashed line near $|\epsilon| = 2 \times 10^{-2}$ indicates extent of critical region.
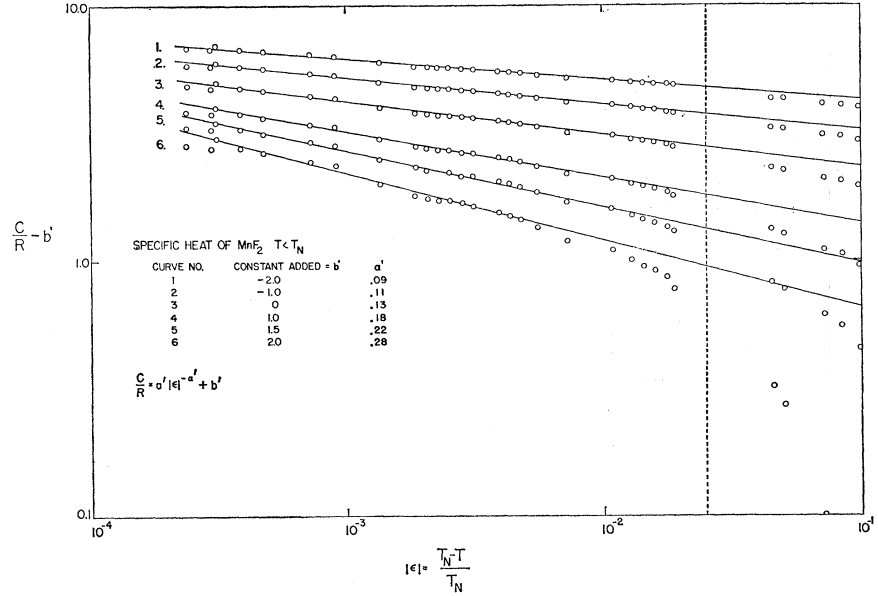
V. CLASSICAL LIQUID–GAS TRANSITIONS

A. Theory

A simplified theory of critical behavior in the liquid-gas transition may be obtained from the Van der Waals equation of state:

$$[P + a(N/V)^2](V - bN) = NkT. \qquad (5.1)$$

When this equation is used in conjunction with the Maxwell equal area construction,[97] results are obtained which are equivalent to those derived from the Landau theory of the second-order phase transition. In particular this approach implies that near the critical point:

(a) At the critical temperature, the density minus the critical density is given by

$$\rho - \rho_c \sim (P - P_c)^{1/3}, \qquad (5.2a)$$

where $P - P_c$ is the deviation of the pressure from its critical value.

(b) On the coexistence curve (see Fig. 9), the densities of gas and liquid are given by

$$\rho_{\text{liquid}} - \rho_c = -(\rho_{\text{gas}} - \rho_c) \sim (T_c - T)^{1/2}. \qquad (5.2b)$$

(c) When $T > T_c$ and $\rho = \rho_c$, the isothermal compressibility K_T diverges as

$$K_T \equiv \rho^{-1}(\partial \rho / \partial P)_T \sim (T - T_c)^{-1}. \qquad (5.2c)$$

(d) There is a similar divergence for $T < T_c$ where

$$K_T \sim (T_c - T)^{-1} \qquad (5.2d)$$

on the coexistence curve.

All these results look like the typical molecular field approximation answers when one identifies[16] the order parameter with $(\rho - \rho_c)$ and the conjugate variable (the analog of the magnetic field) with a quantity proportional to the pressure minus the critical pressure.

A further argument for the identification is provided by the lattice gas model for classical fluids.[98,17] In this

TABLE X. Scaling law comparison.

	$2-\alpha$	$2-\alpha'$	$d\nu$	$d\nu'$	$d\gamma/2-\eta$	$\gamma+2\beta$	$\gamma'+2\beta$	$\beta(\delta+1)$	$y=1/\nu$	Δ[b]
Ferromagnets	1.92 ±0.08	1.92 ±0.08	1.95 ±0.09	···	2.08 ±0.12	1.99 ±0.09	···	1.7 ±0.2	1.54 ±0.07	3.2 ±0.2
Antiferromagnets	1.92 ±0.08	1.92 ±0.08	1.95 ±0.09	···	···	1.96 ±0.10[a]	···	···	1.54 ±0.07	3.2 ±0.2

[a] Here we use the approximation $\gamma \approx 2\nu$.   [b] Calculated from $\Delta = 2d\nu - 2\beta$.
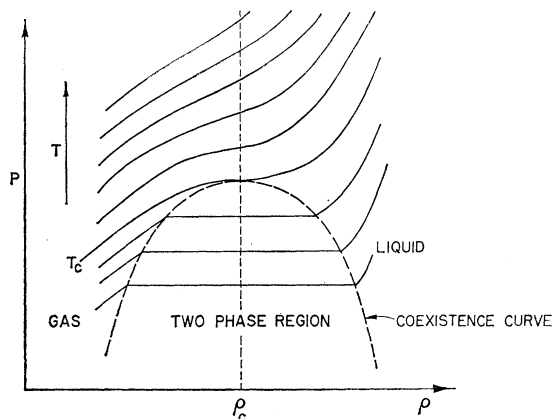
Fig. 9. Schematic pressure vs density diagram near the liquid–gas critical point.

model, the positions of the gas molecules are assumed to take on only discrete values, these values forming a specified lattice. To represent the fact that, in the real fluid, there is a short-range repulsion which keeps the molecules from getting too close to one another, it is assumed that each lattice site can be occupied by at most one molecule. To represent the fact that the real fluid exhibits an attraction between neighboring molecules, the lattice gas model includes an interaction potential which gives a negative contribution to the energy whenever nearest-neighbor sites are occupied.

The lattice gas model has been shown by Lee and Yang[98] to be mathematically identical to the Ising model of ferromagnetic phase transitions. This identity follows since for both models the essential features are a lattice, a nearest-neighbor interaction, and a number for each lattice site which can take on one of two values, i.e., for the Ising model, the z component of the spin

$$\sigma_r = +1 \quad \text{if the spin is up at a site,}$$

$$= -1 \quad \text{if the spin is down at a site,} \qquad (5.3)$$

for the lattice gas the gas density at a lattice site,

$$\rho(\mathbf{r}) = 1 \quad \text{if the site is occupied,}$$

$$= 0 \quad \text{if the site is unoccupied.} \qquad (5.4)$$

According to the above, to obtain a correspondence between the Ising model and the lattice gas model one should make the identification

$$\sigma_r = 2[\rho(\mathbf{r}) - \tfrac{1}{2}]. \qquad (5.5)$$

For the lattice gas model the critical density turns out to be $\tfrac{1}{2}$, so the above statements say that the density minus the critical density plays the role of the magnetization in the lattice gas case. Since there is no difference between up and down magnetization for a ferromagnet we thus have the important quantitative

conclusion that the lattice gas model will predict a perfect symmetry between behavior on the high- and low-density sides of the critical point. For example, if we define β_L and β_G by the requirement that

$$\rho_{\text{liquid}} - \rho_c \sim (-\epsilon)^{\beta_L}$$

$$\rho_{\text{gas}} - \rho_c \sim -(-\epsilon)^{\beta_G} \qquad (5.6)$$

on the coexistence curve, then we know that the lattice gas will give the result $\beta_L = \beta_G$.

A partial list of the corresponding quantities for the two models is given in Table XI. More detailed lists and a derivation of the correspondences are given in Refs. 98 and 17. Thus, a solution for the Ising model, discussed in Sec. IIE can be transcribed into a solution for the lattice gas model. If we then say that the lattice gas model is like the real fluid, we have determined the critical indices for the liquid–gas transition in terms of the indices α, β, γ, etc., for the Ising model. This proposed correspondence between thermodynamic derivatives for the fluid and critical indices for the Ising model is listed in Table XII.

In looking at the experimental data which follow, we focus on the following questions:

Are phase transitions in different fluids essentially similar?

Do they resemble the Ising model's critical behavior? Do they obey the scaling laws?

B. Experiments

In our discussion of experimental data, we concentrate upon the fluids CO_2, Xe, Ar, and O_2 because these are the ones which have been most extensively investigated in the critical region.[99–113] In these one-component systems, the critical point is defined as that temperature and pressure at which the densities of gas and liquid become identical. This point is the top of the coexistence curve of Fig. 9. Table XIII is a list of critical pressures, densities, and temperatures for these four fluids.

TABLE XI. Correspondences between lattice gas model and Ising model.

Ising model	Lattice gas model
Number of up spins	Number of molecules
Partition function	Grand partition function
Number of spins	Volume
Free energy minus magnetic field	Pressure
Magnetization	Density minus critical density
Specific heat C_m	Specific heat C_V

Some of the general difficulties inherent in these measurements may be mentioned. As with second order phase transitions in other materials in other effects, temperature control is critical. In some of the experiments involving the critical points in fluids, the data do not seem to settle down to their asymptotic critical behavior until $\epsilon = (T - T_c)/T_c$ gets smaller than 10^{-2}. A temperature control system must be able to maintain and reproduce temperatures to perhaps one part in 10^4 of T_c in order to provide meaningful data over a two-decade range in ϵ within this critical region. Since this control is most easily achieved near room temperature, the most complete data are available for the classical gases Xe ($T_c = 289.6°K$) and CO_2 ($T_c = 304.0°K$).

Given a good temperature control system, one must next contend with the extremely large compressibilities when critical conditions are approached. Due to the weight of the fluid, critical pressure is realized only

TABLE XII. Definitions of critical indices for liquid–gas transition. If this transition is described correctly by the lattice gas model, α, α', β, γ, γ', and δ all have the same values as in the Ising model.

ϵ	$\epsilon = (T - T_c)/T_c$	
α'	$C_v \sim (-\epsilon)^{-\alpha'}$	$\rho = \rho_c,\ \epsilon < 0$
α	$C_v \sim \epsilon^{-\alpha}$	$\rho = \rho_c,\ \epsilon > 0$
β	$(\rho_L - \rho_G) \sim (-\epsilon)^\beta$	$\epsilon < 0$, coexistence curve.
γ'	$K_T \sim (-\epsilon)^{-\gamma'}$	$\epsilon < 0$, coexistence curve.
γ	$K_T \sim \epsilon^{-\gamma}$	$\rho = \rho_c,\ \epsilon > 0$
δ	$\|P - P_c\| \sim \|\rho - \rho_c\|^\delta$	$T = T_c$
μ	Surface tension $\sim (-\epsilon)^\mu$	$\rho = \rho_c,\ \epsilon < 0$

over a very narrow vertical height range in a sample bomb (in theory, of course, only at a single horizontal plane), and what is measured in a PVT measurement is the average condition of the fluid. This may be quite different from the critical condition unless special precautions are taken, and can lead to a flat top in the coexistence curve[106] (liquid–gas density difference as a function of temperature). One of the most elegant methods of dealing with this was devised by Lorentzen,[105,106] who used a long vertical tube as his cell and measured the density of the fluid as a function of height near the critical region by the refraction of parallel light beams passing through the cell. All critical exponents except α and α' can be determined directly from an experiment of this type.

A further complication arises from the large heat capacity of a fluid near critical conditions.[101,107,108] Equilibration times become very long near the critical point as a result of this, necessitating waits of perhaps days before it is reasonably certain equilibrium conditions have been attained.

TABLE XIII. Critical points of selected fluids.

Gas	P_c	ρ_c	T_c
Xe	57.636 ± 0.115 atm[a]	1.105 g[b]/cm³	$16.590 \pm 0.001°C$[b]
O_2	49.7 atm[c]	0.408 g[d]/cm³	$154.565°K$[d]
Ar	48.34 atm[e]	0.5333 g[f]/cm³	$150.71°K$[e]
CO_2	72.82 atm[g]	0.464 g[h]/cm³	$31.04°C$[g]

[a] Reference 99.
[b] Reference 100.
[c] *Handbook of Chemistry and Physics* (Chemical Rubber Publ. Co., Cleveland, Ohio, 1961).
[d] Reference 101.
[e] Reference 103.
[f] Reference 102.
[g] Reference 104.
[h] Reference 105.

The most accurately determined parameter for the classical gases is β of the coexistence curve. This is determined from the slope of the log–log plot in Fig. 10. Plotted here are the results of four different experiments on CO_2 and Xe over almost a five decade range in ϵ. There is excellent agreement between the data and a line of slope 0.34 over the entire range and for both gases. The data taken by Lorentzen in 1965[106] was shifted vertically to coincide with the other sets; presumably there was a constant factor error in the density of this measurement, for the slope of the line is the same as the rest.

The results for β are summarized in Table XIV. All of this data is consistent with the statement that β is the same for all three fluids. We assume that this is true and take $\beta = 0.346 \pm 0.01$ as the value to be used in further analysis. Notice that this is slightly higher than the lattice gas value, $\beta = 0.31 \pm 0.01$.

The index δ can be calculated directly from the PVT data of Habgood and Schneider.[99] Our analysis is shown in Fig. 11 together with the results of Widom and Rice's[109] analysis of the data of Ref. 104. Since the Xe data cover a larger range, we use it to define the "best value" of δ listed in Table XV. There is a significant deviation from the lattice gas.
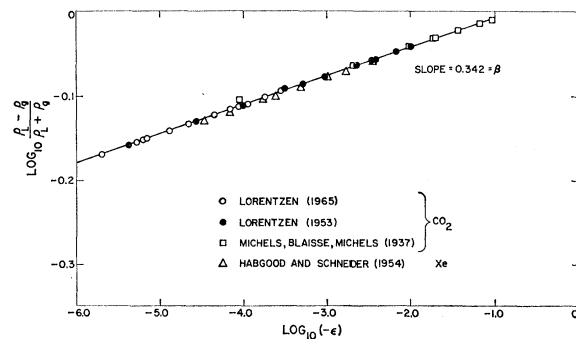

FIG. 10. Coexistence curve data for CO_2 and Xe. The critical index $\beta \approx 0.34$ over almost five decades in ϵ.

TABLE XIV. Summary table for β.

Fluid	β	Reference	Range of ϵ
Xe	0.350 ± 0.015	99	$4\times10^{-5}<-\epsilon<4\times10^{-3}$
Ar	0.4 ± 0.2	103	$6\times10^{-5}<-\epsilon<8\times10^{-3}$
Ar	0.33 ± 0.05	103	$8\times10^{-3}<-\epsilon<10^{-1}$
CO_2	0.344 ± 0.01	105	$4\times10^{-6}<-\epsilon<10^{-1}$
"Best value"	0.346 ± 0.01		
Lattice gas	0.313 ± 0.004	Table III	

We employ three different modes of analysis to determine γ for Xe, CO_2, and Ar. For Xe, we employ the PVT data of Habgood and Schneider.[99] When these data are differentiated they give the K_T values plotted in Fig. 12. Then, γ is the slope of this curve. Unfortunately, this evaluation of γ is rather ambiguous because of the relatively small range of ϵ and the apparent change in slope at $\epsilon\approx10^{-3}$. However, the data points for the higher values of ϵ, $\epsilon\sim10^{-3}$, are believed to be more reliable than those for lower values, $\epsilon\sim10^{-4}$. If we weight the data in this way, we would conclude $\gamma=1.3\pm0.2$. Results for γ and γ' are listed in Tables XVI and XVII.

An application of the Ornstein–Zernike theory to the critical opalescence scattering of x rays in the critical region[16] has been used by Thomas and Schmidt[110] to calculate γ for argon. The theory is probably accurate only outside the critical region, but gives the result that reciprocal intensity plotted against momentum transfer at a constant temperature yields straight lines whose zero intercept with the ordinate is proportional to the reciprocal of the isothermal compressibility.[16] These intercepts as a function of temperature are plotted in Fig. 13.
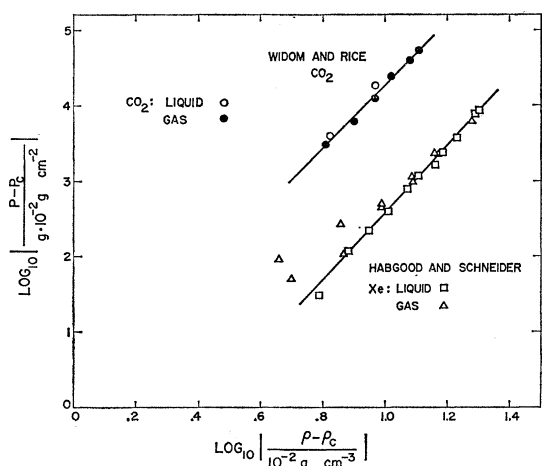
For CO_2, γ may be obtained from the data of Michels, Blaisse, and Michels[104] and of Lorentzen.[105,106] Lorentzen measured the refraction R as a function of height x for light which traversed his tube. At the critical density, R as a function of x shows a point of inflection and a slope $\tan \alpha = dx/dR$ which is a function of temperature. Since R is proportional to the density,

$$(\tan \alpha)^{-1}\sim d\rho/dx=\partial\rho/\partial P \mid_T (dP/dx). \quad (5.8)$$

At the critical density, $dP/dx=-\rho_c g$ is a constant and

$$\tan \alpha\sim K_T^{-1}\sim\epsilon^\gamma. \quad (5.9)$$

Heller[111] has analyzed Lorentzen's 1953 data[105] in conjunction with the results of Michel et $al.$[104] He concludes in CO_2 that $\gamma=1.37\pm0.2$ for $10^{-5}<\epsilon<10^{-2}$ and $\gamma'=1.0\pm0.3$.

Lorentzen's more recent results[106] give a rather different answer. Figure 14 shows that $\tan \alpha$ is quite closely linear in ϵ. Thus, γ appears to be equal to 1.0 ± 0.1 in the range $10^{-6}<\epsilon<2\times10^{-5}$. These results tend to suggest that γ changes at $\epsilon\sim10^{-5}$ in CO_2. However, experimental difficulties are severe when ϵ is
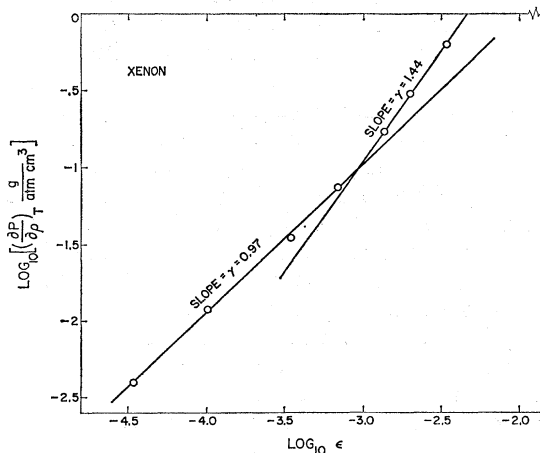

FIG. 11. Data from which the critical index δ is determined.

FIG. 12. PVT data for Xenon from which the critical index γ can be determined.

TABLE XV. Summary of results for δ.

Fluid	Value of δ	Reference	Range of variables
Xe	4.4±0.4	99	$6\times10^{-2}<\mid(\rho-\rho_c)/\rho_c\mid<2\times10^{-1}$
CO_2	4.2	109	$1.4\times10^{-1}<\mid(\rho-\rho_c)/\rho_c\mid<1.8\times10^{-1}$
"Best value"	4.4±0.4		
Lattice gas	5.2±0.15	Table III	

as small as 10^{-5} and perhaps Lorentzen's later results should be discounted for this reason.

There is another reason for concern about using the data in Fig. 14 for finding γ. We want to know K_T for a homogeneous system. But, gravitational effects necessarily produce a pressure gradient of magnitude

$$dP/dx=\rho_c g. \quad (5.10)$$

Can this gradient affect the measured value of K_T appreciably? Let us assume that the long-range correlations in the system basically average the pressure over one coherence length. Then we might expect that the result of the gradient (5.10) could be roughly equivalent to producing a deviation $P-P_c$ of the order

$$\mid P-P_c\mid\sim\rho_c g\xi. \quad (5.11)$$

If this is large enough to push the system away from the critical point, we can evaluate K_T^{-1} by setting $\epsilon=0$. At $\epsilon=0$, the Widom and Rice[109] analysis of CO_2 data indicates

$$(\rho-\rho_c)/\rho_c\sim[(P-P_c)/P_c]^{1/\delta} \quad \delta\approx4.2.$$

Then

$$\frac{\rho_c}{P_c}\frac{dP}{d\rho}\bigg|_T\sim\delta\left(\frac{P-P_c}{P_c}\right)^{1/\delta}\sim\left(\frac{\rho_c g\xi}{P_c}\right)^{1-1/\delta} \quad (5.12)$$

In the last step of (5.12) we have inserted the effective pressure deviation of Eq. (5.11). If this pressure deviation is small, we should expect that the contribution (5.12) to the inverse susceptibility is much smaller than the $P=P_c$ value which is roughly

evaluable[111,105,104]

$$(\rho_c/P_c)(\partial P/\partial\rho)\mid_T\approx10^2\epsilon^\gamma \quad \gamma\approx1.4. \quad (5.13)$$

If we are to neglect the effects of gravity gradients, we should require that the contribution (5.12) to $dP/d\rho\mid_T$ be much less than the contribution (5.13). We evaluate this requirement by guessing ξ from the Ising model results as

$$\xi=(M/\rho_c)^{1/3}\epsilon^{-\nu} \quad \nu\approx0.6,$$

where $(M/\rho_c)^{1/3}$ is the average distance between CO_2 molecules. Then our requirement for neglecting gravitational effects in CO_2 becomes

$$\epsilon\gg10^{-5}. \quad (5.14)$$

The same procedure applied to Xe indicates that the gravitational pressure gradients are negligible for

$$\epsilon\gg3\times10^{-5}. \quad (5.15)$$

Since Eq. (5.14) indicates that pressure gradients might be important in determining γ in Fig. 14, we omit the data of Ref. 106 from further analysis.

The variation of heat capacity with ϵ has been measured most accurately [102,110] for Ar and O_2. The data for Ar for $T<T_c$ are given in Fig. 15. In this log–log plot, we have subtracted constants from C_v/R so that we may fit C_v to a form

$$C_v/R=a\epsilon^{-\alpha}+b \quad \text{for } T>T_c$$

$$=a'(-\epsilon)^{-\alpha'}+b' \quad \text{for } T<T_c.$$

The values of b' are given on each curve together with the value of α' which best fits for that value of b'. A

TABLE XVI. Value of γ.

Fluid	Value of γ	Reference	Range of ϵ	Comments
Xe	1.3±0.2	99	$3\times10^{-4}<\epsilon<3\times10^{-3}$	$\epsilon\leq10^{-4}$ neglected
Ar	0.6±0.2	110	$3\times10^{-3}<\epsilon<6\times10^{-2}$	Is extrapolation procedure right?
CO_2	1.37±0.2	105, 104, 111	$10^{-5}<\epsilon<10^{-2}$	
CO_2	1.0±0.1	106	$10^{-6}<\epsilon<2\times10^{-5}$	Perhaps pressure gradients are important
"Best value"	1.37±0.2			
Lattice gas	1.250±0.001	Table III		

TABLE XVII. Values of γ'.

Fluid	Value of γ'	Reference	Range of ϵ	Comments
Ar	1.1 ± 0.2	110	$6\times10^{-4}<-\epsilon<6\times10^{-2}$	Is extrapolation procedure right?
CO_2	1.0 ± 0.3	105, 104, 111	$\epsilon\approx3\times10^{-2}$ $\epsilon\approx3\times10^{-5}$ $\epsilon\approx3\times10^{-6}$	If pressure gradients are important, this analysis gives no information.
"Best value"	1.0 ± 0.3			Very little information
Lattice gas	1.31 ± 0.05	Table III		

good fit cannot be obtained for α' as large as 0.37, but any value of α' in the region $0\le\alpha'\le.25$ can, with a suitable value of b', fit the data. Of course, $\alpha'=0$ corresponds to a logarithmic singularity in C_v.

For $T>T_c$, a similar plot indicates that any value of α in the range $0<\alpha<0.4$ fits the data for O_2. These results are summarized in Tables XVIII and XIX.

We consider one more critical index, μ, which is defined by the statement that in the two-phase region the surface tension is proportional to $(-\epsilon)^\mu$. Guggenheim[114] quotes results which tend to indicate $\mu\approx1.22$ but a recent analysis by Buff, Lovett, and Stillinger[115] of the data of Atack and Rice[116] on cyclohexene-aniline and of Stansfield[117] on argon and nitrogen gives $\mu\approx1.27\pm0.02$. We use this value in our scaling law analysis.

C. Use of Inequalities

In this analysis, γ' is the quantity with the largest uncertainty. Fortunately there is an exact[118a,16] thermodynamic inequality which we can use to tie down γ'.

FIG. 13. Determination of γ and γ' from x-ray scattering data for Argon. However, the Ornstein–Zernike theory used in the data analysis may not be valid in the critical region.

This inequality is

$$2\beta+\gamma'\ge2-\alpha' \qquad \text{(for } \alpha'>0). \qquad (5.16)$$

When we substitute the known values of β and α', we see that

$$\gamma'\ge1.19\pm0.12.$$

Another exact inequality[118b]

$$\beta(\delta+1)\ge2-\alpha' \qquad \text{(for } \alpha'>0) \qquad (5.17)$$

implies

$$\delta\ge4.45\pm0.4.$$

This does not provide any useful limitations on δ but at least it indicates that the experimental results for δ are not wildly wrong.
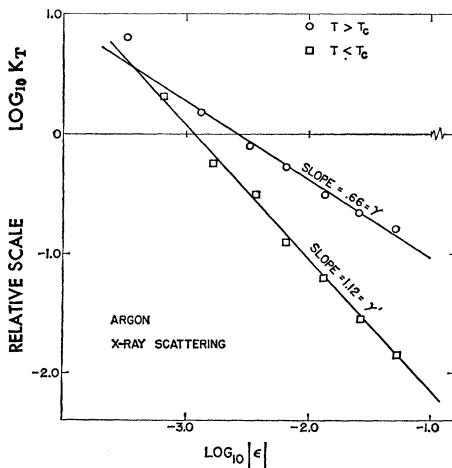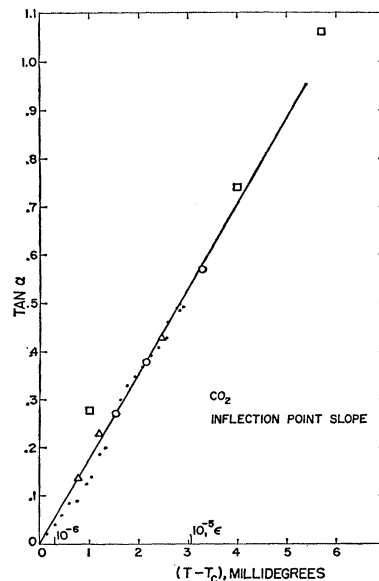

FIG. 14. Lorentzen's data near T_c for angle of refraction α of light passing through CO_2. Tan $\alpha\sim\epsilon^\gamma$.
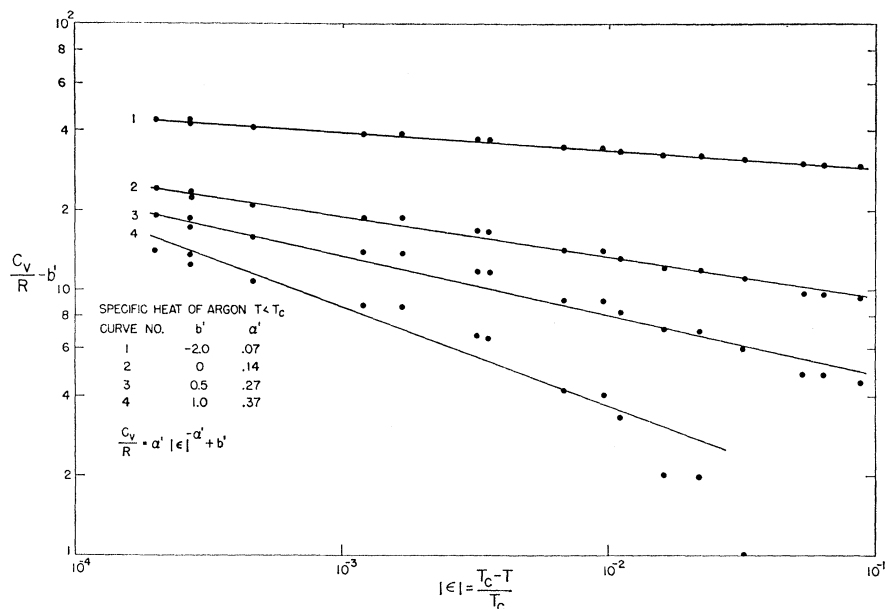
FIG. 15. Three-parameter fits to the specific heat of argon.

D. Comparison with Scaling Laws

According to the discussion in Sec. III, the scaling law approach would predict that the following combinations of indices were all precisely equal: $2-\alpha$, $2-\alpha'$, $\gamma+2\beta$, $\gamma'+2\beta$, $\beta(\delta+1)$. Widom, in his development[33] of the ideas we have called scaling laws, also proposed that the surface tension index, μ, should be equal to $d/(d-1) = \frac{2}{3}$ times these other combinations of indices. In Table XX are listed the quantities which the scaling laws would equate, and it is seen that they are roughly equal. In fact, the results presented here agree within experimental error with the conclusions of the scaling law theory.

From the value of μ in Table XX, we derive the basic scaling law quantity $y=\nu^{-1}=(d-1)/\mu$ as

$$y=1.57\pm0.03. \tag{5.18}$$

The other basic parameter of the scaling law analysis

is $\Delta=2d/y-2\beta$, which turns out to be

$$\Delta=3.12\pm0.1. \tag{5.19}$$

These values of y and Δ are in agreement with the Ising model results (Table IV). However, the difference between the experimental value of $\beta=0.346\pm0.01$ and the Ising model value of $\beta=0.31\pm0.01$ indicates that real fluids and the Ising model show slightly different critical behavior.

VI. THE LIQUID GAS PHASE TRANSITION IN QUANTUM LIQUIDS

A. Theory

Some experimental evidence (see Sec. VIB) tends to indicate that the critical exponents characterizing the liquid–gas phase transition are markedly different for the light substances He, H_2, and D_2, when compared with the results for the heavier elements Xe, Kr, Ar, N_2, O_2, and Ne. If we assume for the moment, that the experiments are correct in indicating this difference, then we must look for an additional parameter which

TABLE XVIII. Values of α'. The experimental numbers are the maximum value of α' which appear consonant with our three parameter fit of the experimental data. Any smaller value of α', including $\alpha'=0$ (logarithmic singularity) will also fit the data.

Fluid	Value of α'	Reference	Range of ϵ
Xe	$<0.2\pm0.1$	112	$5\times10^{-3}<-\epsilon<3\times10^{-2}$
O_2	<0.25	101	$4\times10^{-4}<-\epsilon<1.4\times10^{-2}$
Ar	<0.25	102	$2\times10^{-4}<-\epsilon<10^{-1}$
CO_2	$<0.1\pm0.5$	113	$3\times10^{-3}<-\epsilon<2\times10^{-2}$
"Best value"	0.12 ± 0.12		
Lattice gas	$0.07^{+0.16}_{-0.04}$	Table III	

TABLE XIX. Values of α. All the data are consistent with α being as small as zero.

Fluid	Value of α	Reference	Range of ϵ
O_2	$\alpha<0.4$	101	$3\times10^{-5}<\epsilon<4\times10^{-2}$
Ar	$\alpha<0.4$	102	$10^{-4}<\epsilon<2\times10^{-2}$
"Best value"	0.2 ± 0.2		
Lattice gas	0.1 ± 0.1	Table III	

TABLE XX. Comparison with scaling laws. According to the analysis of Sec. III all of these numbers should be equal. The numbers used here are the "best values" of Tables XIV–XIX.

$2-\alpha$	$2-\alpha'$	$\gamma+2\beta$	$\gamma'+2\beta$	$\beta(\delta+1)$	$\frac{3}{2}\mu$
1.8	1.88	2.06	1.7	1.87	1.91
±0.2	±0.12	±0.2	±0.3	±0.14	±0.03

measures quantum behavior. It is quite reasonable to suggest that the different behavior of light gases is a manifestation of the quantum-mechanical dispersion[119] in the position of the molecules, which occurs when the kinetic energy of a molecule is comparable in magtitude to the effective potential energy of that molecule. To give this statement some quantitative substance we discuss the law of corresponding states as formulated by de Boer.[120] First we consider the classical problem.

Assume that the interaction between molecules is given by the potential energy $\rho(r)$. We can apply a law of corresponding states if, for different fluids

$$\rho(r) = \Delta f(r/\sigma),\qquad(6.1)$$

where $f(x)$ has the same form for all fluids. Then Δ and σ represent the characteristic energy and length for the fluid in question. We may compare different fluids by using the reduced variables:

$$T^* = kT/\Delta,\qquad V^* = V/N\sigma^3,\qquad P^* = P\sigma^3/\Delta.\qquad(6.2)$$

Since the potential energy function, (6.1), determines all of the statistical properties of a classical fluid, P^* should be the very same function of V^* and T^* for different fluids as long as quantum corrections are unimportant. Table XXI indicates that the critical reduced pressure, temperature, and specific volume are found to be nearly the same for the heavier fluids.

However, the kinetic energy is important in quantum statistical mechanics. If a particle is localized in a volume of order σ^3, it has a kinetic energy of the order

$$\hbar^2/m\sigma^2\qquad(6.3)$$

according to the uncertainly principle. The size of the quantum correction can be estimated by comparing

(6.3) with the typical potential energy Δ. The ratio of these two energies

$$(\Lambda^*)^2 \equiv \hbar^2/m\sigma^2\Delta\qquad(6.4)$$

is a dimensionless measure of the importance of quantum effects in the liquid–gas transition. Table XXI shows that as Λ^* becomes larger than unity (in H_2, He^4, and He^3), the critical pressure, temperature, and volume deviate from their classical values.

The classical phase transition has been compared with the Ising model via the lattice gas (see Sec. V). Because, in the quantum case the Hamiltonian contains noncommuting terms, it is attractive to compare the quantum liquid–gas transition with a magnetic situation in which there are spins with noncommuting components. This has been done by Matsubara and Matsuda,[121] and Zilsel.[122] These models suggest that the quantum transition is like a ferromagnetic transition in an anisotropic situation, in which the zero field magnetization can only point in the z direction. Once more, one can identify $(\rho-\rho_c)$ with the z component of the magnetization. Since not very much is known about highly anisotropic ferromagnets near the critical point, it is difficult to judge the correctness of these models. However one point stands out clearly. Since the magnet shows complete symmetry between spin up and spin down, these quantum lattice gas models would predict a complete symmetry between liquid and vapor.

B. Experiment

The specific heats of both helium three and helium four have been measured by Moldover and Little.[124] We have fit their data to a formula:

$$C = a\epsilon^{-\alpha} + b\qquad\text{for } T > T_c$$
$$= a'(-\epsilon)^{-\alpha'} + b'\quad\text{for } T < T_c\qquad(6.5)$$

with a, a', b, and b' being adjustable parameters. The data for He^4 and some fits to it are shown in Fig. 16. We would conclude that α' lies between 0.0 (logarithmic singularity) and 0.2 and α between 0.0 and 0.3. However, this conclusion does not include a possible perturbation produced by gravitational effects. Accord-

TABLE XXI. Experimental values of P_{cr}^*, V_{cr}^*, T_{cr}^*, and Λ^* for substances having the potential energy function (6.1).

	Xe	Kr	Ar	N_2	Ne	H_2	He^4	He^3
P_{cr}^*	0.112	0.117	0.116	0.132	0.114	0.063	0.027	0.014[a]
V_{cr}^*	3.10	3.10	3.12	2.88	3.25	4.29	5.74	7.2[a]
T_{cr}^*	1.26	1.26	1.25	1.30	1.26	0.90	0.51	0.33[a]
Λ^*	0.064	0.102	0.187	0.225	0.591	1.73	2.64	3.05[a]

[a] Computed using present known values of P_{cr}, T_{cr}, and ρ_{cr}[132] and the values of Δ and σ appropriate for He^3 (the same as for He^4).[123] All other numbers are from Ref. 120.
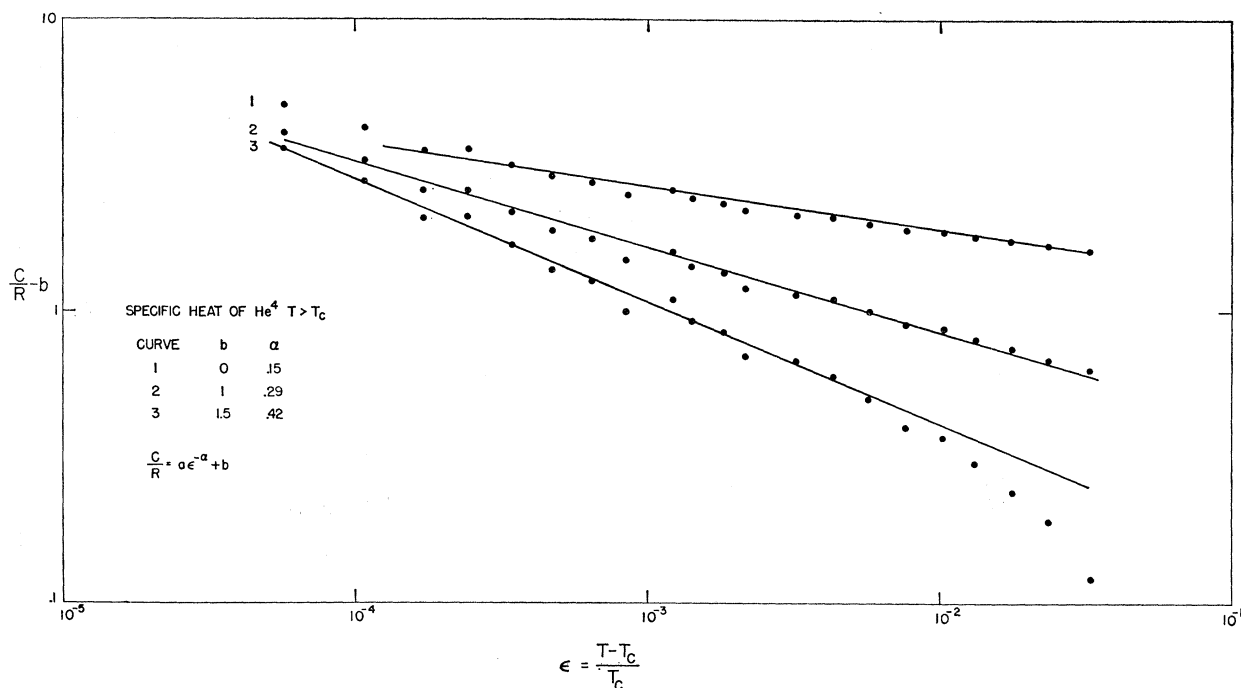
FIG. 16. Three-parameter fits to the specific heat of He⁴ near the liquid-gas transition.

ing to a calculation based on the Landau theory,[125] using the data of Edwards and Woodbury,[126,127] a 1% density variation might exist in this experiment for $\epsilon < 5 \times 10^{-4}$. This could cause a rounding of the specific heat peak.

The order parameter for liquid-gas transitions is $\rho - \rho_c$, and therefore the analog of the magnetization in zero field is just the coexistence curve. For this the relevant critical exponent is β. Edwards and Woodbury[126] measured this for He⁴ by using a Jamin interferometer. They measured the index of refraction of a "slice" of helium 1 mm thick, and from this determined the density using the Lorentz-Lorenz equation. The correction to this equation near the critical point has been estimated to be negligible using a theory of Larson, Mountain, and Zwanzig.[129] The results of this experiment have been fitted to many analytical expressions,[126-128] but for comparison with other data, we have considered only fits of the form

$$(\rho_L - \rho_G)/\rho_c \sim (-\epsilon)^\beta. \qquad (6.6)$$

Unfortunately, this experiment does not permit an unambiguous conclusion about β. By varying T_c and the assumed size of the critical region within reasonable limits it appears possible to obtain fits for values of β which are in the range 0.40 to 0.50.

The results of recent measurements by Roach and Douglass[130] are that $\beta = 0.35 \pm 0.01$ for $4 \times 10^{-4} < (-\epsilon) < 2 \times 10^{-2}$. They measured the dielectric con-

stant of helium between two capacitor plates, and obtained the density using the Clausius-Mosotti equation. Edwards[131] has also repeated his measurements, and his recent result is that $\beta = 0.37 \pm 0.02$ for $2 \times 10^{-4} < (-\epsilon) < 10^{-2}$. Thus it appears that β is about the same in He⁴ as in the classical gases (see Table XXII).

The coexistence curve for He³ has been determined by Sherman[132] by measuring the pressure of the vapor as a function of temperature using a constant volume bomb filled to 23 different densities. The pressure-temperature relations obtained in this way are nearly linear, and are extrapolated to the known vapor-pressure curve to give temperature-density data. This method has the advantage of giving the shape of the entire PVT surface near the critical point, and thus giving more information than just β. Furthermore, the effect of gravity and the infinite compressibility is avoided, since no part of the fluid is at the critical point. However, the extrapolation to the vapor curve is questionable, since it is not known definitely that the isochores (constant volume) continue to be linear in the immediate neighborhood of the critical point.[133]

We fit Sherman's data for $2.5 \times 10^{-2} < (-\epsilon) < 2.5 \times 10^{-1}$ with $\beta = 0.36 \pm 0.02$. Since his published data include only two data points for $(-\epsilon) < 2.5 \times 10^{-2}$, we do not feel justified in estimating β in this region. However, the data suggest a possible increase in β towards 0.5.

TABLE XXII. Comparison of quantum and classical fluids.

	He³	He⁴	H₂	Classical gases[h]
α	$\lesssim 0.3$[a] $4\times10^{-4}<\epsilon<2\times10^{-2}$	$\lesssim 0.3$[a] $10^{-4}<\epsilon<3\times10^{-2}$		$\lesssim 0.4$
α'	$\lesssim 0.2$[a] $2\times10^{-4}<-\epsilon<3\times10^{-2}$	$\lesssim 0.2$[a] $2\times10^{-4}<-\epsilon<3\times10^{-2}$		$\lesssim 0.25$
β	0.36 ± 0.02[b] $2.5\times10^{-2}<(-\epsilon)<2.5\times10^{-1}$	0.352 ± 0.004[c] $4\times10^{-4}<(-\epsilon)<2\times10^{-2}$	0.36 ± 0.01[d] $10^{-2}<(-\epsilon)<?$	0.35 ± 0.01
γ	1.09 ± 0.05[b] $?<\epsilon<?$			1.37 ± 0.2
γ' (gas)	1.00 ± 0.05[b] $?<-\epsilon<?$			1.0 ± 0.3
γ' (liquid)	1.18 ± 0.10 $?<-\epsilon<?$			1.0 ± 0.3
δ	3.5 ± 0.1[e] $0.17<\mid(\rho-\rho_c)/\rho_c\mid<1.0$		4.2[f] $0.67<\mid(\rho-\rho_c)/\rho_c\mid<1.57$	4.4 ± 0.4
μ			1.25 ± 0.02[g] $4\times10^{-2}<(-\epsilon)<4\times10^{-1}$	1.27 ± 0.02

[a] Reference 124.
[b] Reference 132.
[c] Reference 130.
[d] Reference 135.
[e] Reference 136.
[f] References 109, 137.
[g] Reference 139.
[h] See Tables XI–XXII.

Fisher[134] proposed an explanation for the apparent ϵ dependence of β which was noted by Sherman. He suggested that the variation in β might reflect the behavior of a system in which quantum corrections are not very large. Then relatively far from T_c, for large ϵ, we should expect classical behavior—$\beta\approx\frac{1}{3}$. Nearer T_c, the more delicate quantum effects take over and β changes its value to one which is characteristic of a quantum system.

However this apparent ϵ dependence of β seems very questionable in view of the recent results for He⁴, for as Roach and Douglass[130] point out, β seems to be independent of Λ^*, the quantum correction parameter, over the range $0.06<\Lambda^*<2.6$ (Xe to He⁴), so that β would have to change very rapidly over the range $2.6<\Lambda^*<3.1$ (He⁴ to He³) to explain the apparent[132] $\beta\approx0.48$ in He³.

The coexistence curve for hydrogen has been determined by the isochoric method,[135] and the data can be fit with $\beta=0.36\pm0.01$ for $\epsilon>10^{-2}$. There is an indication that β becomes larger (≈0.50) for $\epsilon<10^{-2}$, but this might be due to the effect of gravity.

Next consider the isothermal compressibility:

$$\chi=\partial\langle p\rangle/\partial h\mid_\epsilon=\partial(\rho-\rho_c)/\partial\mu\mid_\epsilon=\rho^2 K_T\sim\epsilon^{-\gamma}. \qquad (6.7)$$

The only available compressibility data are those of Sherman,[132] who found $\gamma=1.09\pm0.05$. Below the phase separation γ' is evaluated along the two branches of the coexistence curve. This yields two different γ' values:

$$\gamma_G=1.00\pm0.05 \quad \text{(gas)}$$

$$\gamma_L=1.18\pm0.10 \quad \text{(liquid)}.$$

These values of γ are obtained from derivatives of PVT data, so they necessarily have large uncertainty. Also uncertain are the size of the critical region and the extrapolation procedure to the coexistence curve. In view of these difficulties one must conclude that a definitive measurement of γ probably requires data closer to the coexistence curve and for smaller values of ϵ.

The shape of the critical isotherm is characterized by the exponent δ.

$$\mid(P-P_c)/P_c\mid=A\mid(\rho-\rho_c)/\rho_c\mid^\delta \qquad \text{at } \epsilon=0. \qquad (6.8)$$

By interpolating the data to the critical isotherm to obtain the density as a function of pressure, Sherman[132] finds $\delta=3.4\pm0.2$. Chase and Zimmerman[136] measured δ more directly by measuring the dielectric constant of He³ as a function of pressure at $T=3.324°K$. Then using the Clausius–Mossotti relation to find the density, they determined $\delta=3.5\pm0.1$. Their data indicate that the coefficient A in Eq. (6.8), is twice as great for the high-density fluid as that for the low-density fluid. The exact ratio depends on the value of the critical density used in Eq. (6.8) but for reasonable values of ρ_c, the ratio is near 2. This difference between high and low density is also seen in Sherman's determination of γ^L and γ^G. This behavior contradicts one of the assumptions in the lattice gas model: that there is symmetry between vapor and liquid. If we were seeing here the true critical behavior this would be strong evidence against the applicability of the lattice gas model to these phase transitions. However, the sparse data for γ and the fact that measurements for

δ were carried out for relatively large values of $| (\rho - \rho_c)/\rho_c |$ prevent the formation of firm conclusions about these critical exponents.

The shape of the critical isotherm for H_2 has been calculated from the data of Johnson, Keller, and Friedman[137] by Widom and Rice,[109] who found $\delta = 4.2$. However, these data required a fairly long extrapolation to obtain δ,[138] which may therefore be unreliable.

Finally, the critical index μ, which relates the surface tension of a liquid drop to $T - T_c$ as surface tension $\sim (-\epsilon)^\mu$, has been measured for H_2 by Blagoi and Pashkov.[139] Their result is $\mu = 1.25$ in the range $4 \times 10^{-2} < -\epsilon < 4 \times 10^{-1}$.

C. Summary and Comparison with Classical Fluids

The results are summarized in Table XXII. Because of the inherent difficulties in these experiments and because of the uncertainty in the size of the critical region all these results, except β for He^4 and the α's, should perhaps be considered to be provisional.

For comparison we list in Table XXII the "best values" for classical fluids as determined in Sec. V. There is no strong indication that the quantum fluids behave differently than classical fluids near the critical point. There are not yet sufficient data to make a scaling law comparison meaningful.

VII. SUPERFLUIDS

A. Order Parameter for this Transition

In the superfluid transition, a finite fraction of the entire number of helium atoms all fall into the very same quantum state.[140,141] The order parameter for this transition is then the wave function of this special state, which we write as $\langle \psi(r) \rangle$. Since this wave function is complex, we have here a two-component critical order parameter. Thus, the behavior of the superfluid might well be different from the liquid–gas transition, in which the order parameter has but a single component. In fact, the superfluid should be most like a hypothetical ferromagnet in which the magnetization can point with equal facility in an entire plane.[142] Unfortunately, we know of no ferromagnet with such an easy plane of magnetization.

Because the order parameter in the superfluid is so special, there is an especial difficulty in learning about this transition: we do not have experimental control over the thermodynamic conjugate to the order parameter. In fact, this conjugate is always zero. Hence, we cannot measure the derivative of the order parameter with respect to its conjugate—the analog to the magnetic susceptibility—in the superfluid case. Similarly, we have no experimental way of finding the (order-parameter)–(order-parameter) correlation function

$$g(r, r') = \langle \psi^+(r')\psi(r) \rangle \qquad (7.1)$$
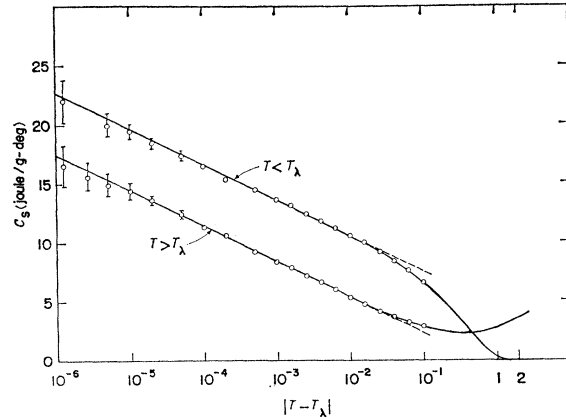
which is the one-particle density matrix.

FIG. 17. Experimental specific heat of liquid He^4 near the superfluid (λ) transition.

B. Experimental Results

Since we cannot vary the variable we have been calling h, the conjugate to the order parameter, any specific heat measured in helium is C at constant h. Far and away the best measurement of C_h has been done by Buckingham, Fairbank, and Kellers,[143] who find C_h along the vapor pressure line for helium. Their results, shown in Fig. 17, indicate a logarithmic divergence in C_h over four decades of ϵ. It seems quite plausible that the divergence is truly logarithmic, i.e., $\alpha = \alpha' = 0$, so that

$$C_h = -A \log | \epsilon | + B \qquad \text{for } \epsilon > 0$$

$$= -A' \log | \epsilon | + B' \qquad \text{for } \epsilon < 0.$$

Also, within experimental error $A = A'$. This is another piece of evidence in support of the scaling law idea, since the scaling laws predict that when there is a logarithmic singularity A must equal A'.

Another piece of useful information is provided by a measurement of the superfluid density ρ_s just below T_c. The definition of ρ_s is the statement that, when the superfluid is moving with velocity v_s, the flow of mass is given by a current

$$\mathbf{g} = \rho_s \mathbf{v}_s. \qquad (7.2)$$

The most accurate critical data for ρ_s are provided by the experiment of Clow and Reppy[144] (Fig. 18) and that of Tyson and Douglass[145] which give

$$\rho_s \sim (-\epsilon)^\zeta \qquad (7.3)$$

$$\zeta = 0.666 \pm 0.006 \qquad \text{for } 3 \times 10^{-5} < -\epsilon \lesssim 10^{-1}. \qquad (7.4)$$

C. Scaling Law for ρ_s

In the relevant molecular field theory, the Landau–Ginzburg approach, ρ_s is simply proportional to the
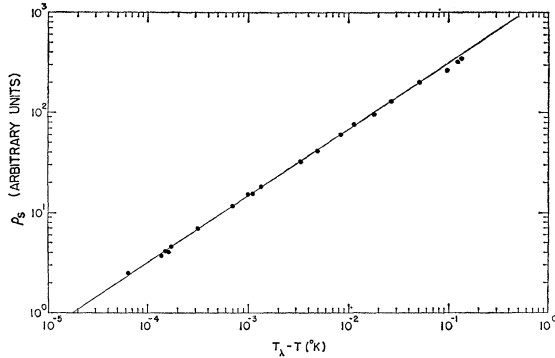
FIG. 18. Superfluid density of liquid He^4 just below T_λ.

order parameter squared

$$\rho_s \sim |\langle\psi\rangle|^2. \tag{7.5}$$

Then, if $\langle\psi\rangle$ goes to zero as $(-\epsilon)^\beta$, Eq. (7.4) would imply $\beta = \frac{1}{3} \pm 0.003$, in agreement with the value for MnF$_2$.

However, Josephson[146] has argued that there is no particular reason for believing that the molecular field result, (7.5), should be correct near the λ point. [In particular he suggests that an extra factor proportional to $(-\epsilon)^{-\eta\gamma'}$ should appear on the right-hand side of Eq. (7.5). Then he uses the scaling laws to replace $2\beta - \eta\gamma'$ by $(d-2)(2-\alpha)/d$.] He concludes, in fact, that $\zeta = \frac{2}{3}$ is a direct consequence of the scaling law arguments and the fact that the specific heat singularity gives $\alpha = 0$.

His argument is based upon the fact that superfluid flow arises from a gradient of the phase of $\langle\psi(r)\rangle$. In fact, v_s is derived from this phase via[141]

$$m v_s(r) = i^{-1}\nabla\langle\psi(r)\rangle/\langle\psi(r)\rangle \tag{7.6}$$

for situations in which the magnitude of $\langle\psi(r)\rangle$ does not vary in space. However, if the superfluid is moving slowly, the free energy per unit volume has the form

$$g(\epsilon, v_s) = g(\epsilon, 0) + \tfrac{1}{2}\rho_s v_s^2, \tag{7.7}$$

where the second term is just the kinetic energy of the superfluid in motion.

Equations (7.6) and (7.7) are definitions of ρ_s and v_s. We now use these definitions in conjunction with scaling law arguments to find ζ. To do this, the kinetic energy term is rewritten with the aid of (7.3) and (7.6) as

$$\tfrac{1}{2}\rho_s v_s^2 \sim (-\epsilon)^\zeta [\ |\nabla\langle\psi(r)\rangle|^2/|\langle\psi(r)\rangle|^2]. \tag{7.8}$$

However, under the scaling law transformations

$$r \to r/L$$

$$\epsilon \to \bar\epsilon = \epsilon L^y \tag{7.9}$$

any singular term in the free energy density is scaled by a factor of L^d [cf. Eq. (3.3)]. In our case, the $(-\epsilon)^\zeta$ in (7.8) introduces a factor of $L^{\zeta y}$ and the gradients introduce two factors of L when the expression 7.8 is scaled. Thus we must have

$$L^d = L^{2+\zeta y}$$

or

$$\zeta = (d-2)/y. \tag{7.10}$$

But, according to Eq. (3.9c)

$$d/y = 2 - \alpha \tag{7.11}$$

so that (7.10) reduces to

$$\zeta = [(d-2)/d](2-\alpha). \tag{7.12}$$

Since we are working in a three-dimensional system, $d = 3$ and from the specific heat experiments $\alpha = 0$. Thus, the scaling laws give $\zeta = \frac{2}{3}$, in agreement with experiment.

For a two-dimensional system (7.12) reduces to the strange result $\zeta = 0$. This would be rather difficult to justify were it not for the fact that there exist theoretical arguments[147] which tend to show that the superfluid transition does not take place or does not have a finite order parameter in a two-dimensional system.

D. Perturbation Theoretic Approach

Patashinskii and Pokrovskii[148] have discussed the nature of the critical singularity near the λ point of helium by attempting to sum the perturbation theory expansion for the one-particle Green's density matrix (7.1). They conclude that the specific heat and $(\partial n/\partial\mu)_T$ should diverge as $\log|\epsilon|$. This conclusion apparently agrees with experiment.[143] However, there have been several objections to this theory. At many points in their work, these authors have to guess the form of functions. They indicate that their guesses might be mutually consistent, but it is not clear that the guesses are correct. Furthermore, Abe[149] has extended their methods to the Ising model. He obtains results which are in clear disagreement with the known Ising model answers. For example, Abe finds $\eta = 1$ in two dimensions and $\eta = \frac{1}{2}$ in three dimensions. The correct answers for these cases are, respectively, $\eta = \frac{1}{4}$ and $\eta = 0.056 \pm 0.008$. (See Table III). This disagreement is one more argument against the theory of Patashinskii and Pokrovskii.

VIII. FERROELECTRIC TRANSITIONS

The ferroelectric transition is accompanied by a drastic change of the lattice structure and thus we always have a strong coupling between elastic, piezo-electric and ferroelectric phenomena of the crystal.[150] Stresses due to lattice imperfections, external forces and domain-clamping, influence the Landau theory

parameters, thus producing an uncontrollable shift and smearing-out of the thermodynamic functions.

For these reasons one generally uses data with $\epsilon > 10^{-3}$ to determine the exponents α, β, and γ, obtaining agreement with the predictions of the phenomenological theory. Measurements of η and ν are not known.

Measurements of γ have been performed[151] for tri-glycine sulfate, KH_2PO_4 and the upper Curie point of Rochelle salt down to values for ϵ of 2×10^{-4}, 8×10^{-4}, and 4×10^{-4}, respectively. In all cases $\gamma = 1$ within the experimental uncertainties of 2%. Hence the critical fluctuations have no influence on γ even for such small values of ϵ.

For temperatures below the lower Curie point in Rochelle salt, Craig[151] has found for the interval $4 \times 10^{-4} < |\epsilon| < 5 \times 10^{-2}$, $\gamma' = 1.23 \pm 0.02$. The phase of the crystal is antiferroelectric there, and thus we must not expect to have the same critical region there as for temperatures near the upper transition point.

None of the other thermodynamic functions has been determined yet with the same accuracy as the values for χ. Thus we are not able to check the predictions of the scaling laws.

There are λ-shaped peaks in the specific heat of e.g., KH_2PO_4,[152] NH_4HSO_4[153] and Rochelle salt.[154] But the reported results do not allow a qualitative conclusion about the details of the singularity.

After having replotted Stephenson and Hooley's data, Grindlay[155] has pointed out that there are indications in favor of the existence of a logarithmic singularity in the specific heat of KH_2PO_4. For $0.6 < |T - T_c| < 5.3(T_c = 127.97°K)$ he obtained $A = 1.2 \pm 0.3$ and $A' = 14.2 \pm 1.4$. This statement cannot be accepted as a disproof of (3.11) for two reasons. Firstly, the discussed values for ϵ are possibly too large to get correct asymptotic data. One also would like to have more than 5 experimental points to determine the A's. Secondly, if one looks very close to the "critical point," one notices that the transition is actually first order.[151] So we have to expect a smeared out peak in the specific heat due to the latent heat of the transition. This peak has nothing to do with critical behavior. Furthermore the critical temperature T_c, seen in the normal phase, is lower than the critical temperature T_c', seen in the ordered state. T_c is the lowest temperature for an undercooling of the paraelectric state, while T_c' is the highest temperature for a superheating of the ferroelectric phase. T_c is[151] $121.062°K$; T_c' is not known. Grindlay's fit depends sensitively on the value of T_c. The assumption that his critical temperature is T_c' can explain qualitatively why A is too small compared with A'.

REFERENCES

* A. P. Sloan Foundation Fellow.

† Stipendiat der Clemens Plassman-Stiftung. On leave from the Max Planck-Institut fur Physik und Astrophysik, Munich, Germany.

‡ Work supported in part by the Advanced Research Projects Agency under Contract ARPA SD-131 and the National Science Foundation Grant NSF GP-4937.

1 *Proceedings of the International Conference on Phenomena near Critical Points*, Washington (1965) NBS Misc. Publication #273.

2 J. Appl. Phys. **37**, No. 3 (March 1966).

3 R. Brout, *Phase Transitions* (W. A. Benjamin, Inc., New York, 1965), discusses this concept of an order parameter in detail.

4 P. W. Anderson, Rev. Mod. Phys. **38**, 298 (1966) discusses the meaning of the order parameter in the superfluid and superconducting transitions.

5 L. D. Landau and E. M. Lifshitz, *Statistical Physics* (Pergamon Press, London, 1958), Chap. 14.

6 This is readily derived by writing the Hamiltonian as $H = H_0 - \int d\mathbf{r} p(\mathbf{r}) h(\mathbf{r})$, using $\langle p(\mathbf{r}) \rangle = \mathrm{Tr}\, p(\mathbf{r}) e^{-\beta H}/\mathrm{Tr}\, e^{-\beta H}$, letting $h(\mathbf{r}) \rightarrow h(\mathbf{r}) + \delta h(\mathbf{r})$, and expanding to first order in $\delta h(\mathbf{r})$.

7 These applications of ideas equivalent to the Landau theory are described in Brout's book (Ref. 3).

8 The Ginzburg–Landau equations for a superconductor are described in E. A. Lynton, *Superconductivity* (John Wiley & Sons, Inc., New York, 1964), Chap. 5. The analogous equations for superfluids, the Gross-Pitaevskii equations, are discussed in E. P. Gross, J. Math. Phys. **4**, 195 (1963).

9 L. Onsager, Phys. Rev. **65**, 117 (1944).

10 C. N. Yang, Phys. Rev. **85**, 808 (1952); T. Schultz, D. Mattis, and E. Lieb, Rev. Mod. Phys. **36**, 856 (1964); G. V. Ryazanov, Zh. Eksperim. i Teor. Fiz. **49**, 1134 (1965) [English transl.: Soviet Phys.—JETP **22**, 789 (1966)].

11 L. P. Kadanoff, Nuovo Cimento **44B**, 276 (1966).

12 T. T. Wu, Phys. Rev. **149**, 380 (1966).

13 C. Domb (Advan. in Phys.) Phil. Mag. Suppl. **9**, 151 (1960); G. F. Newell and E. W. Montroll, Rev. Mod. Phys. **25**, 253 (1953).

14 D. Mattis, *The Theory of Magnetism* (Harper and Row, New York, 1965), Chap. 9; K. Huang, *Statistical Mechanics* (John Wiley & Sons, Inc., New York, 1965), Chap. 16.

15 M. E. Fisher, J. Math. Phys. **4**, 278 (1963).

16 M. E. Fisher, J. Math. Phys. **5**, 944 (1964).

17 M. E. Fisher, in *Lectures in Theoretical Physics* (University of Colorado Press, Boulder, Colo. 1965), Vol. VII, Part C, p. 1.

18 Unpublished calculations by one of the authors (R. Hecht). He finds that $G_{EE}(\epsilon R) \sim [K_1^2(|\epsilon|R) - K_0^2(|\epsilon|R)]$, where K_n is the modified Bessel function of the second kind (see, e.g., H. B. Dwight, *Tables of Integrals and Other Mathematical Data* (The Macmillan Co., New York, 1965) and

$$G_{\sigma E}(\epsilon R) \sim \int_{2\epsilon r}^{\infty} x^{-2} e^{-x} dx.$$

19 This result is derivable from Eqs. (43), (71), and (72) of B. Kaufman and L. Onsager, Phys. Rev. **76**, 1244 (1949). See also Ref. 12.

20 V. L. Ginzburg, Fiz. Tverd. Tela. **2**, 2031 (1960) [English transl.: Soviet Phys.—Solid State **2**, 1824 (1960)].

21 A. P. Levanyuk, Zh. Eksperim. i Teor. Fiz. **36**, 810 (1959) [English transl.: Soviet Phys.—JETP **9**, 571 (1959)].

22 M. Kac, G. E. Uhlenbeck, and P. C. Hemmer, J. Math. Phys. **4**, 216 (1963); G. E. Uhlenbeck, P. C. Hemmer, and M. Kac, *ibid.* **4**, 229 (1963); P. C. Hemmer, M. Kac, and G. E. Uhlenbeck, *ibid.* **5**, 60 (1964); P. C. Hemmer, *ibid.* **5**, 75 (1964).

23 N. G. van Kempen, Phys. Rev. **135**, A362 (1964).

24 J. L. Lebowitz and O. Penrose, J. Math. Phys. **7**, 98 (1966).

25 See Lynton, Ref. 8.

26 D. Thouless, Ann. Phys. **10**, 553 (1960); E. G. Batyev, A. Z. Patashinskii, and V. L. Pokrovskii, Zh. Eksperim. i Teor. Fiz. **46**, 2093 (1964) [English transl.: Soviet Phys.—JETP **19**, 1412 (1964)].

27 J. S. Shier and D. M. Ginsberg, Phys. Rev. **147**, 384 (1966).

28 H. A. Gersch, C. G. Shull, and M. K. Wilkinson, Phys. Rev. **103**, 525 (1956).

29 D. G. Howard, B. D. Dunlap, and J. G. Dash, Phys. Rev. Letters **15**, 628 (1965).

30 G. Gorodetsky, S. Shtrikman, and D. Treves, Solid State Commun. **4**, 147 (1966).

31 L. P. Kadanoff, Physics **2**, 263 (1966).

32 C. Domb and D. L. Hunter, Proc. Phys. Soc. (London) **86**, 1147 (1965); C. Domb, Ann. Acad. Sci. Fennicae, Ser. A, VI, Physica 210, Helsinki (1966).

[33] M. E. Fisher, J. Appl. Phys. **38**, 981 (1967).

[34] (a) B. Widom, J. Chem. Phys. **43**, 3892 (1965); (b) **43**, 3898 (1965).

[35] M. E. Fisher, Proceedings of the University of Kentucky Centennial Conference on Phase Transitions (March 1965).

[36] A. Z. Patashinskii and V. L. Pokrovskii, Zh. Eksperim. i Teor. Fiz. **50**, 439 (1966) [English transl.: Soviet Phys.—JETP **23**, 292 (1966)].

[37] J. W. Essam and M. E. Fisher, J. Chem. Phys. **39**, 842 (1963).

[38] G. E. Uhlenbeck and P. C. Hemmer, *Proceedings of the International Symposium on Statistical Mechanics and Thermodynamics, Aachen, Germany* (North-Holland Publ. Co., Amsterdam, 1965).

[39] The arguments given here are somewhat similar to arguments which have been given by Buckingham in Ref. 1.

[40] Reference 31 gives a particular description for the construction of μ_a as being proportional to the sum over the entire cell of σ_r. This particular description is not necessary for the conclusions drawn here so that we do not include it here. In other respects, our arguments follow quite closely those of Ref. 31.

[41] The cancellation of L in all physical quantities is a very stringent requirement upon the theory. In particular, it is hard to see how (3.13) could be generalized and still allow L to cancel out of $\langle \sigma_r \rangle$.

[42] A relation of this kind occurs in Ref. 37 which proposes $\alpha' + 2\beta + \gamma' = 2$. In Ref. 35, Fisher argues for Eq. (3.9) on the basis of Frenkel, Band, and Bijl's theory of condensation. In Ref. 34b, Widom derives all these relations from an assumption which is equivalent to the assertion that Eq. (3.7) is correct. Uhlenbeck and Hemmer, in Ref. 38, have given thermodynamic arguments in favor of $\gamma + 2\beta = 2$ when $\alpha = \alpha' = 0$.

[43] The result $d\nu = 2 - \alpha$ was suggested by Widom in Ref. 34a. A result of this type follows from an argument given by A. B. Pippard, Proc. Roy. Soc. London **A216**, 547 (1953).

[44] W. P. Wolf and A. F. G. Wyatt, Phys. Rev. Letters **13**, 368 (1964).

[45] A. R. Miedema, H. van Kempen, and W. J. Huiskamp, Physica **29**, 1266 (1963).

[46] A. H. Cooke, D. T. Edmonds, C. B. P. Finn, and W. P. Wolf, J. Phys. Soc. Japan **17**, Suppl. B-1, 481 (1962).

[47] G. A. Baker, H. E. Gilbert, J. Eve, and G. S. Rushbrooke, Phys. Letters **20**, 146 (1966).

[48] C. Domb and M. F. Sykes, Phys. Rev. **128**, 168 (1962); J. Gammel, W. Marshall, and L. Morgan, Proc. Roy. Soc. (London) **275**, 257 (1963).

[49] P. J. Wood and G. S. Rushbrooke, Phys. Rev. Letters **17**, 307 (1966).

[50] See Ref. 17, p. 121.

[51] P. Heller and G.B. Benedek, Phys. Rev. Letters **8**, 428 (1962).

[52] E. Sawatzky and M. Bloom, Can. J. Phys. **42**, 657 (1964).

[53] J. E. Noakes, N. E. Tornberg, and A. Arrott, J. Appl. Phys. **37**, 1264 (1966).

[54] P. Heller, Phys. Rev. **146**, 403 (1966).

[55] O. K. Rice, J. Chem. Phys. **22**, 1535 (1954); O. K. Rice, J. Phys. Chem. **64**, 976 (1960); R. A. Farrell and P. H. E. Meijer, Physica **31**, 725 (1965); C. P. Bean and D. S. Rodbell, Phys. Rev. **126**, 104 (1962); D. C. Mattis and T. D. Schultz, *ibid.* **129**, 175 (1963).

[56] S. Arajs and R. V. Colvin, J. Appl. Phys. **35**, 2424 (1964).

[57] G. Develey, Compt. Rend. **260**, 4951 (1965).

[58] P. Weiss and R. Forrer, Ann. Phys. (Paris) **5**, 153 (1926). These data were analyzed near T_c by J. S. Kouvel and M. E. Fisher, Phys. Rev. **136**, A1626 (1964); and also in Ref. 62.

[59] S. Arajs, J. Appl. Phys. **36**, 1136 (1965).

[60] C. D. Graham, J. Appl. Phys. **36**, 1135 (1965).

[61] R. V. Colvin and S. Arajs, J. Phys. Chem. Solids **26**, 435 (1965).

[62] J. S. Kouvel and D. S. Rodbell, Phys. Rev. Letters **18**, 215 (1967).

[63] H. E. Stanley and T. A. Kaplan, J. Appl. Phys. **38**, 975, 977 (1967).

[64] L. Van Hove, Phys. Rev. **35**, 1374 (1954).

[65] P. G. DeGennes, in *Magnetism*, G. T. Rado and H. Suhl, Eds. (Academic Press Inc., New York, 1963), Vol. III.

[66] L. Passell, K. Blinowski, T. Brun, and P. Nielsen, Phys. Rev. **139**, A1866 (1965).

[67] See Ref. 3, Chap. 2.

[68] T. Riste and A. Wanic, Phys. Letters **16**, 231 (1965).

[69] M. J. Cooper and R. Nathans, J. Appl. Phys. **37**, 1041 (1966).

[70] G. T. Freeman and R. E. Watson, in *Magnetism*, G. T. Rado and H. Suhl, Eds. (Academic Press Inc., New York, 1965), Vol. IIA.

[71] R. S. Preston, S. S. Hanna, and J. Heberle, Phys. Rev. **128**, 2207 (1962).

[72] For example, see J. G. Dash, B. D. Dunlap, and D. G. Howard, Phys. Rev. **141**, 376 (1966).

[73] H. B. Callen, D. Hone, and A. Heeger, Phys. Letters **17**, 233 (1965).

[74] D. Hone, H. Callen, and L. R. Walker, Phys. Rev. **144**, 283 (1966).

[75] E. Callen and H. Callen, J. Appl. Phys. **36**, 1140 (1965).

[75a] A. Arrott *et al.*, J. Appl. Phys. **38**, 969 (1967).

[76] N. J. Poulis and G. E. G. Hardeman, Physica **19**, 391 (1953).

[77] W. Van der Lugt and N. J. Poulis, Physica **26**, 917 (1960).

[77a] *Note added in proof.* More recent work by Preston has filled in more data points for iron with $-\epsilon \gtrsim 10^{-3}$. These results seem consistent with $\beta \approx 1/3$. We wish to thank Dr. Preston for sending us his work prior to publication.

[78] H. H. Potter, Proc. Roy. Soc. (London) **146**, 362 (1934).

[79] P. Heller and G. B. Benedek, Phys. Rev. Letters **14**, 71 (1965).

[80] M. Eibschutz, S. Shtrikman, and D. Treves, Solid State Commun. **4**, 141 (1966).

[81] S. D. Senturia and G. B. Benedek, Phys. Rev. Letters **17**, 475 (1966).

[82] For example, if we use the scaling law relation $2\beta + \gamma = 2 - \alpha$ and Kouvel and Rodbell's data [Ref. 62 and our Eqs. (4.2)] for Ni ($\beta = 0.42$, $\gamma = 1.35$) and CrO_2 ($\beta = 0.33$, $\gamma = 1.6$) we find $\alpha = -0.19$ for Ni and $\alpha = -0.26$ for CrO_2.

[83] A. B. Pippard, *The Elements of Classical Thermodynamics* (Cambridge University Press, Cambridge, England, 1964), Chap. 9.

[84] J. Skalyo, Jr., and S. A. Friedberg, Phys. Rev. Letters **13**, 133 (1964).

[85] A. R. Miedema, R. F. Wielinga, and W. J. Huiskamp, Phys. Letters **17**, 87 (1965).

[86] D. T. Teaney, Phys. Rev. Letters **14**, 898 (1965).

[87] See Table VII.

[88] See Table V.

[89] S. A. Friedberg and J. D. Wasscher, Physica **19**, 1072 (1953).

[90] D. T. Teaney, V. L. Moruzzi, and B. E. Argyle, J. Appl. Phys. **37**, 1122 (1966).

[91] Ya. A. Kraftmakher and T. Yu. Romashina, Fiz. Tverd. Tela **7**, 3532 (1965) [English transl.: Soviet Phys.—Solid State **7**, 2040 (1966)].

[92] A. R. Miedema, R. F. Wielinga, and W. J. Huiskamp, Physica **31**, 1234 (1965).

[93] Ya. A. Kraftmakher, Fiz. Tverd. Tela **8**, 1306 (1966) [English transl.: Soviet Phys.—Solid State **8**, 1048 (1966)].

[94] M. E. Fisher, Proc. Roy. Soc. (London) **A254**, 66 (1960).

[95] B. E. Keen, D. Landau, B. Schneider, and W. P. Wolf, J. Appl. Phys. **37**, 1120 (1966).

[96] W. H. M. Voorhoeve and Z. Dokopuil, Physica **27**, 777 (1961).

[97] See Ref. 3, Chap. 3.

[98] T. D. Lee and C. N. Yang, Phys. Rev. **87**, 410 (1952); see also Ref. 14, K. Huang.

[99] H. W. Habgood and W. G. Schneider, Can. J. Chem. **32**, 98 (1954).

[100] M. A. Weinberger and W. G. Schneider, Can. J. Chem. **30**, 422 (1952).

[101] A. V. Voronel', Yu. R. Chashkin, V. A. Popov, and V. G. Simkin, Zh. Eksperim. i Teor. Fiz. **45**, 828 (1963) [English transl.: Soviet Phys.—JETP **18**, 568 (1964)].

[102] A. V. Voronel', V. G. Snigirev, and Yu. R. Chashkin, Zh. Eksperim. i Teor. Fiz. **48**, 981 (1964) [English transl.: Soviet Phys.—JETP **21**, 653 (1965)].

[103] A. Michels, J. M. Levelt, and W. de Graaf, Physica **24**, 659 (1958); A. Michels, J. M. Levelt, and G. J. Walkers, *ibid.* **24**, 769 (1958).

[104] A. Michels, B. Blaisse, and C. Michels, Proc. Roy. Soc. (London) **160A**, 358 (1937).

[105] H. L. Lorentzen, Acta Chem. Scand. **7**, 1335 (1953).

[106] H. L. Lorentzen, *Statistical Mechanics of Equilibrium and Nonequilibrium* (North-Holland Publ. Co., Amsterdam, 1965), p. 262.

[107] M. I. Bagatskii, A. V. Voronel', and V. G. Gusak, Zh. Eksperim. i Teor. Fiz. **43**, 728 (1962) [English transl.: Soviet Phys.—JETP **16**, 517 (1963)].

[108] Kh. I. Amirkhonov and I. G. Gurvich, Dokl. Akad. Nauk. SSSR **91**, 221 (1953); Chemical Abstracts **48**, 13363g (1954).

[109] B. Widom and O. K. Rice, J. Chem. Phys. **23**, 1250 (1955).

[110] J. E. Thomas and P. W. Schmidt, J. Chem. Phys. **39**, 2506 (1963).

[111] P. Heller, to be published in a review for Rept. Progr. Phys. We wish to thank Dr. Heller for telling us of his results prior to publication.

[112] A. V. Voronel', Zh. Fiz. Khimii **35**, 958 (1961).

[113] A. Michels and J. Strijland, Physica **18**, 613 (1952).

[114] E. A. Guggenheim, J. Chem. Phys. **13**, 253 (1945).

[115] F. P. Buff and R. A. Lovett, *Simple Dense Fluids: Data and Theory*, H. L. Frisch and Z. W. Salsburg, Eds. (Academic Press Inc., New York, to be published); F. P. Buff, R. A. Lovett, and F. H. Stillinger, Jr., Phys. Rev. Letters **15**, 621 (1965), footnote 7.

[116] D. Atack and O. K. Rice, Discussions Faraday Soc. **15**, 210 (1953).

[117] D. Stansfield, Proc. Phys. Soc. (London) **72**, 854 (1958).

[118] (a) G. S. Rushbrooke, J. Chem. Phys. **39**, 842 (1963); (b) R. B. Griffiths, *ibid*. **43**, 1958 (1965).

[119] C. N. Yang and C. P. Yang, Phys. Rev. Letters **13**, 303 (1964).

[120] J. deBoer, Physica **14**, 139 (1948).

[121] T. Matsubara and H. Matsuda, Progr. Theoret. Phys. (Kyoto) **16**, 569 (1956).

[122] P. R. Zilsel, Phys. Rev. Letters **15**, 476 (1965).

[123] J. deBoer and R. J. Lunbeck, Physica **14**, 318 and 510 (1948).

[124] M. R. Moldover and W. A. Little, Phys. Rev. Letters **15**, 54 (1965).

[125] A. V. Voronel' and M. Sh. Giterman, Zh. Eksperim. i Teor. Fiz. **39**, 1162 (1960) [English transl.: Soviet Phys.—JETP **12**, 809 (1961)].

[126] M. H. Edwards and P. W. C. Woodbury, Phys. Rev. **129**, 1911 (1963).

[127] L. Tisza and C. E. Chase, Phys. Rev. Letters **15**, 4 (1965).

[128] M. H. Edwards, Phys. Rev. Letters **15**, 349 (1965); L. Mistura and D. Sette, *ibid*. **16**, 268 (1966).

[129] S. Y. Larsen, R. D. Mountain, and R. Zwanzig, J. Chem. Phys. **42**, 2187 (1965).

[130] P. R. Roach and D. H. Douglass, Jr., Phys. Rev. Letters **17**, 1083 (1966). We wish to thank Dr. Roach and Dr. Douglass for sending us a preprint of their work.

[131] M. H. Edwards, *Proceedings of the Tenth International Conference on Low Temperature Physics, Moscow*, 1966 (to be published). We wish to thank Dr. Edwards for sending us a preprint of his work.

[132] R. H. Sherman, Phys. Rev. Letters **15**, 141 (1965).

[133] B. Widom (private communication).

[134] M. E. Fisher, Phys. Rev. Letters **16**, 11 (1966).

[135] H. M. Roder, D. E. Diller, L. A. Weber, and R. D. Goodwin, Cryogenics **3**, 16 (1965).

[136] C. E. Chase and G. O. Zimmerman, Phys. Rev. Letters **15**, 483 (1965).

[137] H. S. Johnson, W. E. Keller, and A. Friedman, J. Am. Chem. Soc. **76**, 1482 (1954).

[138] R. H. Sherman and E. F. Hammel, Phys. Rev. Letters **15**, 9 (1965).

[139] Yu. P. Blagoi and V. V. Poshkov, Zh. Eksperim. i Teor. Fiz. **49**, 1453 (1965) [English transl.: Soviet Phys.—JETP **22**, 999 (1966)].

[140] O. Penrose and L. Onsager, Phys. Rev. **104**, 576 (1956).

[141] D. Pines, *Theory of Quantum Liquids* (W. A. Benjamin, Inc., New York, to be published), Vol. 2.

[142] V. G. Vaks and A. I. Larkin, Zh. Eksperim. i Teor. Fiz. **49**, 975 (1965) [English transl.: Soviet Phys.—JETP **22**, 678 (1966)].

[143] C. F. Kellers, thesis, Duke University (1960). M. J. Buckingham and W. M. Fairbank, *Progress in Low Temperature Physics* (North-Holland Publ. Co., Amsterdam, 1961), Vol. III.

[144] J. R. Clow and J. D. Reppy, Phys. Rev. Letters **16**, 887 (1966).

[145] J. A. Tyson and D. H. Douglass, Jr., Phys. Rev. Letters **17**, 472 (1966); and erratum, Phys. Rev. Letters **17**, 622 (1966).

[146] B. D. Josephson, Phys. Letters **21**, 608 (1966).

[147] T. M. Rice, Phys. Rev. **140**, A1889 (1965). J. W. Kane, thesis, Univ. of Illinois (1966).

[148] A. Z. Patashinskii and V. L. Pokrovskii, Zh. Eksperim. i Teor. Fiz. **46**, 994 (1964) [English transl.: Soviet Phys.—JETP **19**, 677 (1964)].

[149] R. Abe, Progr. Theoret. Phys. (Kyoto) **33**, 600 (1965).

[150] P. W. Forsbergh, Jr., in *Handbuch der Physik*, S. Flügge, Ed. (Springer-Verlag, Berlin, 1956), Vol. 17; W. Känzig, in *Solid State Physics*, F. Seitz and D. Turnbull, Eds. (Academic Press Inc., New York, 1957), Vol. 4, p. 1; F. Jona and A. Shirane, *Ferroelectric Crystals* (The Macmillan Co., New York, 1962).

[151] P. P. Craig, Phys. Letters **20**, 140 (1966).

[152] C. C. Stephenson and J. A. Hooley, J. Am. Chem. Soc. **66**, 1397 (1944).

[153] B. A. Strukov and M. N. Danilychewa, Fiz. Tverd. Tela. **5**, 1724 (1963) [English transl.: Soviet Phys.—Solid State **5**, 1253 (1963)].

[154] A. A. Rusterhold, Helv. Phys. Acta **8**, 39 (1935).

[155] J. Grindlay, Phys. Rev. **139**, A1603 (1965).